

## **Fate of production in the Arctic seasonal ice zone**

*An investigation of suspended biomass, vertical export and the impact of grazers during the onset of the spring bloom north of Svalbard*

—  
**Christine Dybwad**

*BIO-3950 Master thesis in Biology, May 2016*



**Frontpage:** Sediment trap ascending through the sea ice. ©Christine Dybwad 2015

## **Acknowledgements**

First and foremost, I would like to thank my supervisor, Marit Reigstad. Not only have you given me the amazing opportunity of joining an exciting international and interdisciplinary project where I was able to test my strengths and learn from others, but you have also taught me to trust in my independent capabilities and to guide my scattered ideas into constructive interpretation. Your endless enthusiasm and evident passion for ecosystem functions and interactions are an inspiration to me, and I thank you for the hours of fascinating discussion, concerning everything from ecological processes occurring under sea ice to animal cognition.

Furthermore, I want to thank Maeve McGovern for the hours of good company, filtration and copepod sorting during the expedition. Thanks also goes to Achim Randelhoff, Felix Lauber, Sarah Zwicker, Thomas Krumpfen and all the others who helped with deployment and retrieval of the sediment traps, especially when they had to be deployed through the sea ice (definitely not a one woman job!). Thank you Hauke Flores for the help in the collection of zooplankton and discussion of abundances at the sea ice stations.

Thanks goes to Sigrid Øygarden for help in the lab, Svein Kristiansen for the nutrient analysis, and Sandra Murawski and Barbara Niehoff for the *Calanus* spp. abundances. Gratitude goes to my brilliant sister, Henriette Dybwad, for the company during some of the fluorescence and FP measurements, and for proofreading.

Finally, thank you to my amazing friends and family, without whose continuous support I would not be where I am today – both mentally and physically.

*Tromsø, 2016*

Christine Dybwad



## Abstract

In the Arctic Ocean, biological productivity is largely determined by sea ice, making the seasonal sea ice zone (SSIZ) its most productive region. The current study is a combined investigation of the suspended biomass, vertical export of organic material, and potential retention processes by zooplankton, during a crucial period of bloom development in the Eurasian SSIZ north of Svalbard, where few studies have previously been done. To evaluate the magnitude and composition of the bloom and subsequent vertical export, short-term sediment traps, at five depths between 30 and 200m, were deployed at eight sea ice stations. Daily patterns of chlorophyll *a*, particulate organic carbon (POC) and contribution of zooplankton fecal pellets (FP) were discovered in distinct assemblages – conditions ranging from pre- to mid-bloom development. Daily loss rates of POC increased from 0.6 to 2.7% as the bloom progressed from a pre- to mid-bloom phase, but the vertical carbon export rates in the shallower depths exceeded those in the deeper layers as the bloom developed accordingly. Phytoplankton carbon (PPC) was found to be a more important component to the vertical POC flux than FP carbon (FPC), especially as the bloom progressed. PPC and FPC contributed 5-75% and 0.5-24% to POC export respectively. The contribution of FPC flux to total POC flux was found to be in line with previous studies, revealing that the relative contribution FPC flux to vertical carbon export is variable but may diminish northward with the SSIZ. The impact of grazers was further investigated through FP production experiments of key *Calanus* species. The proportion of *Calanus finmarchicus* community-produced FPC exported to 40m decreased from 36% to 4% from early- to mid-bloom conditions, suggesting stronger zooplankton-mediated retention as the bloom intensifies. Additionally, under slower bloom development, grazers appeared to be effectively controlling and inhibiting the accumulation of biogenic biomass and subsequent vertical flux. The current study reveals that the northern ice-covered Barents Sea shelf break can provide comparable vertical export rates of organic material during the spring bloom to the productive and shallower central Barents Sea.

*Keywords:* Bloom development, vertical carbon export, fecal pellet retention, seasonal sea ice zone, Eurasian Arctic

## Abbreviations

AO	Arctic Ocean
ArW	Arctic water
AW	Atlantic water
AWI	Alfred-Wegener Institute, Bremerhaven
BSB	Barents Sea branch
Chl <i>a</i>	Chlorophyll <i>a</i>
CTD/RO	Conductivity, temperature, depth-Rosette water sampler system
CV	Copepodite stage V
F	Female
FP	Fecal pellets
FPC	Fecal pellet carbon
FPV	Fecal pellet volume
POC	Particulate organic carbon
PON	Particulate organic nitrogen
PPC	Phytoplankton carbon
S	Salinity
SSIZ	Seasonal sea ice zone
T	Temperature
UiT	University of Tromsø, The Arctic University of Norway
WSB	West Spitzbergen branch
YP	Yermak Plateau

# Table of Contents

<b>ACKNOWLEDGEMENTS</b> .....	<b>1</b>
<b>ABSTRACT</b> .....	<b>3</b>
<b>ABBREVIATIONS</b> .....	<b>4</b>
<b>1. INTRODUCTION</b> .....	<b>6</b>
<b>2. MATERIALS AND METHODS</b> .....	<b>8</b>
2.1 STUDY PERIOD AND AREA CHARACTERISTICS .....	8
2.2 PHYSICAL CHARACTERISTICS OF SNOW, ICE AND WATER COLUMN .....	10
2.3 WATER COLUMN SAMPLING / SUSPENDED PROFILES .....	11
2.4 VERTICAL EXPORT.....	12
2.5 ZOOPLANKTON FP PRODUCTION EXPERIMENTS .....	13
2.6 LABORATORY ANALYSIS.....	14
2.6.1 <i>Nutrients analysis</i> .....	14
2.6.2 <i>Chlorophyll a and phaeopigment analysis</i> .....	14
2.6.3 <i>Particulate organic carbon and nitrogen (POC, PON) analysis</i> .....	15
2.7 FECAL PELLET ENUMERATION AND MEASUREMENTS.....	16
2.8 CALCULATIONS .....	17
2.8.1 <i>Sedimentation rates of chlorophyll a, POC and PON</i> .....	17
2.8.2 <i>Integrated suspended chlorophyll a and POC</i> .....	18
2.8.3 <i>Daily loss rate</i> .....	18
2.8.4 <i>Estimate of Phytoplankton Carbon (PPC)</i> .....	18
2.8.5 <i>Fecal pellet volume and sedimentation rates</i> .....	19
2.8.6 <i>Community FPC production (0-40m)</i> .....	20
2.9 STATISTICAL ANALYSIS .....	21
<b>3. RESULTS</b> .....	<b>22</b>
3.1 PHYSICAL CHARACTERISTICS OF THE SAMPLING AREA .....	22
3.2 BLOOM DEVELOPMENT GROUPING.....	23
3.3 SUSPENDED MATERIAL .....	25
3.4 VERTICAL EXPORT.....	27
3.4.1 <i>Daily chlorophyll a and phaeopigment flux</i> .....	27
3.4.2 <i>Daily POC flux and estimation of PPC contribution</i> .....	29
3.5 INTEGRATED PROFILES AND BIOMASS LOST TO 90M DEPTH .....	31
3.5.1 <i>Integrated biomass and contribution of large cells</i> .....	31
3.5.2 <i>Daily loss rates to 90m depth</i> .....	32
3.6 DAILY FPC FLUX .....	33
3.7 FP PRODUCTION AND COMMUNITY GRAZING .....	35
3.7.1 <i>FP production</i> .....	35
3.7.2 <i>Estimation of Calanus spp. community FP export</i> .....	38
<b>4. DISCUSSION</b> .....	<b>40</b>
4.1 SUCCESSIONAL CHARACTERISTICS OF BLOOM EVENTS AT THE SSIZ .....	40
4.2 VERTICAL EXPORT – FATE OF THE BLOOM .....	42
4.3 IMPACT OF GRAZERS .....	44
4.4 OUTLOOK AND FUTURE WORK.....	48
<b>5. CONCLUSION</b> .....	<b>50</b>
<b>REFERENCES</b> .....	<b>51</b>
<b>APPENDIX</b> .....	<b>58</b>

## 1. Introduction

In the Arctic Ocean, biological productivity and the corresponding ecosystem connections are controlled by the dynamics of the sea ice, as it regulates the light transmission, and stabilization of the water column below it, and thus the nutrient availability (Sakshaug 2004, Boetius *et al.* 2013, Barber *et al.* 2015). The seasonal sea ice zone (SSIZ), which directly experiences the dynamic nature of sea ice throughout the year, is therefore the Arctic Oceans most biologically prominent region but also the fastest changing as a consequence of a warming climate (Wassmann and Reigstad 2011).

The SSIZ is usually characterized by short and intense phytoplankton blooms in the plentiful sunlight of spring/summer (Wassmann *et al.* 1999b, Arrigo *et al.* 2012), and correspondingly very little production during the extremely limited light conditions of winter (Berge *et al.* 2015). The productive season is vital for all life in the Arctic, and consequently, the main source of the carbon produced and exported to the sea floor in the Arctic SSIZ, away from coastal inputs, is phytodetritus (Renaud *et al.* 2008). However, the consumption and remineralization of this source through trophic interactions controls the fate of the bloom and therein the quantity and quality of the organic material exported out of the productive pelagic surface waters (Wassmann *et al.* 2006, Reigstad *et al.* 2008, Tamelander *et al.* 2009). The regulatory processes involved in retention of the export of organic material mostly occur in the upper part of the water column where production accumulates, and very little retention is evoked in waters deeper than 200m (Wassmann *et al.* 2003, Boyd and Trull 2007, Renaud *et al.* 2008). Therefore, high resolution studies of vertical carbon export from the productive upper waters underneath the ice, and the processes that regulate the downward flux in the upper water column, are relevant in understanding the function and potential for carbon sequestration of the SSIZ ecosystem.

Zooplankton play a major role in the regulation of carbon export. Efficient zooplankton grazing reduces the bulk of the bloom available for export, while the production of fast sinking fecal pellets (FP) can enhance the downward flux and carbon sequestration (Wassmann 1998, De La Rocha and Passow 2007). Conversely, grazers can mediate degradation processes and subsequently attenuate the downward flux of organic material, including FP, through physical destruction and ingestion (Turner 2015). In the Barents Sea, FP produced by larger meso- and macrozooplankton were found to contribute an average of 20% to the vertical flux of organic carbon (Wexels Riser *et al.* 2008). Wexels Riser *et al.* (2008) additionally found that the older copepodite stages of *Calanus* spp. contributed most to the flux of FP at the majority of stations, whilst appendicularians and krill FP were found prominent at certain stations and depths. Therefore, the identification of key *Calanus* species and their contribution to the flux of organic material, will aid in the understanding of the



processes involved in carbon sequestration at different stages of the bloom (Noji *et al.* 1999, Wexels Riser *et al.* 2007, Wexels Riser *et al.* 2010).

The current study focuses on the Eurasian and innermost region of the SSIZ, in the late spring – early summer period, where the largest inter-annual variability in productivity takes place (Wassmann *et al.* 2010, Slagstad *et al.* 2015). The area is subject to great but variable impact of advected water masses from the Atlantic (Aagaard *et al.* 1987, Beszczynska-Möller *et al.* 2012), but the influence of advected productivity and fauna on the flux of material is still uncertain (Wassmann *et al.* 2015). Additionally, in 2015, the Arctic experienced the fourth minimum sea ice extent recorded by satellite data, making the study area, as well as the seasonal period, crucial to the melting of the SSIZ (NSIDC).

The research on which this study is based, was part of the international TRANSSIZ (AWI\_PS92\_00) expedition of spring 2015, onboard the German icebreaker RV Polarstern (PS92 – ARK XXIX/1). TRANSSIZ (Transitions in the Arctic Seasonal Sea Ice Zone) was part of the Arctic in Rapid Transition (ART) initiative. This highly interdisciplinary cruise was aimed at enhancing the understanding of the physical, chemical and biological responses of the Arctic ecosystem to the changing climate and sea ice extent. The expedition focused on linking past and present sea ice transitions in the European Arctic through ecological and biogeochemical spring process studies.

With varying physical, biogeochemical and ecological conditions during the onset of the spring bloom, the aim of the study was to:

- Outline successional characteristics that define the vernal bloom at the study region of the SSIZ
- Explore the vertical export and the fate of the bloom with possible retention processes in the study area
- Investigate the contribution from grazers and their impact on vertical flux mediation and retention as the bloom develops

## 2. Materials and methods

### 2.1 Study period and area characteristics

This research was part of the international TRANSSIZ (PS92 – ARK XXIX/1) expedition during spring and early summer of 2015 (May 19 – June 28), onboard the German icebreaker RV Polarstern. During the 6-week expedition to the shelf break and Arctic basin north of Svalbard, eight sea-ice stations were investigated (fig. 1), each approximately 24 hours in duration allowing for the deployment and retrieval of the sediment traps and other ice-related research.

The study area, located north of Svalbard, is situated on and northwest of the Eurasian shelf break of the Arctic Ocean (AO) (fig. 1). This region is in the seasonal sea ice zone (SSIZ), characteristically dominated by first- and second-year ice, as well as drift ice (Peeken 2016). Consequently, the study area is highly exposed to summer sea ice melt due to rising air and water temperatures, leading to shifts in sea ice thickness and extent during the research period (Müller *et al.* 2009, Peeken 2016) (appendix fig. A1).

The SSIZ experiences additional large-scale physical seasonal transitions, such as ice drift and advection of warmer water masses. Vast amounts of AW are forced northwards along the Norwegian coast, after which it splits into separate branches, continuing north through the Barents Sea (Barents Sea Branch (BSB)) (Rudels 2012) and the Fram Strait (West Spitzbergen Branch (WSB)) (Aagaard *et al.* 1987, Walczowski 2013) (fig. 1). Currently the Fram Strait forms the only deep-water connection between the high AO and the North Atlantic, and contributes the greatest inflows of water into the AO (Bluhm *et al.* 2015). Our research was conducted where this AW flows through the eastern Fram Strait (northwest of Svalbard) with the WSB and around the Yermak Plateau (YP) (fig. 1). This area is of particular interest as it is in the so-called Polar domain (Walczowski 2013), in the vicinity of a polar front, where the relatively warm and salty AW (Salinity (S) $>34.92$ , Temperature (T) $>2^{\circ}\text{C}$  (Beszczynska-Möller *et al.* 2012, Walczowski 2013)) is submerged under the cooler and fresher ArW and surface water (S $<34.92$  when cooler than  $2^{\circ}\text{C}$  (Walczowski 2013)). These merging water masses and the intermediate water they form (S $>34.92$  and T $<2^{\circ}\text{C}$  (de Steur *et al.* 2014)) impact both the physical and biological characteristics in the area (Wassmann *et al.* 2015). Moreover, the Yermak Plateau, being a shallower outstretched feature, adds complexity to the area and directs ocean circulation and the distribution of biological communities in this region of the Arctic (Fer *et al.* 2010, Wassmann *et al.* 2015).

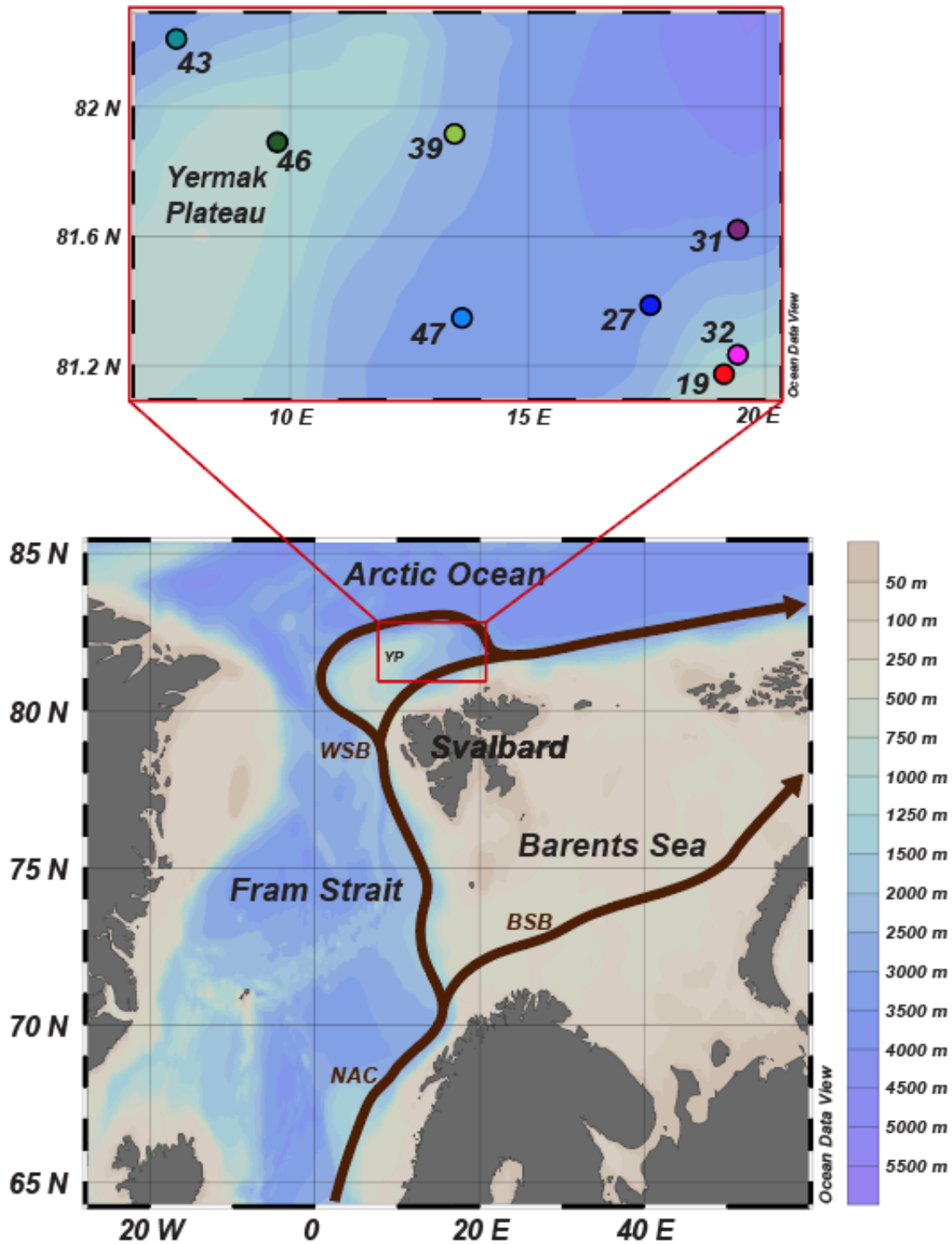


Figure 1. Map showing the western section of the Eurasian Arctic, the Barents Sea and Fram Strait. Inset specifying the locations of the 8 research ice stations. Map includes bathymetric depth gradients (right) and main ocean currents (WSB: West Spitzbergen Branch; BSB: Barents Sea Branch). YP: Yermak Plateau. Note bathymetric depth scale is representative for lower map only.

## 2.2 Physical characteristics of snow, ice and water column

Sea ice thickness and snow measurements were collected at each ice station using ground-based measurements and airborne measurements (AEM Bird) using helicopter surveys. For the purpose of this study, the ground-based measurements were used, where snow and sea ice thickness was measured using a MagnaProbe and GEM-2 survey, as well as with ROV transects. Ice cover (scale 0-10, 10 being complete cover) was estimated from sea ice observations made from the RV Polarstern bridge, using the software based protocol ASSIST. The sea ice physical characteristics of the stations were measured and provided by the sea ice physics team onboard (table 1).

Conductivity, temperature, depth (CTD) profiles were made at each station using a Sea-Bird Electronics Inc. SBE911+ CTD-Rosette water sampler system (CTD/RO). A Fluorescence sensor (WETLabs ECO-AAFL/FL) was mounted on the CTD/RO, providing instant measurements of fluorescent algal material in the water column, and used to estimate chlorophyll *a* maximum depths (table 1). The CTD/RO was run, and the data provided, by the physical oceanographic team onboard.

All physical information is taken from the PS92 cruise report (Peeken 2016) and from personal observations made at the ice stations (table 1).

Table 1. Station dates, locations and bottom depths (m), as well as sea ice cover of the area (/10), mean snow and ice thickness (m), CTD/RO estimated depth of chlorophyll *a* maxima (m), and sediment trap deployment positions and times (in hours) during the TRANSSIZ expedition of 2015.

Station	Date (Start)	Position (Lat. °N, Long. °E) (Start)	Station depth (m)	Ice cover (/10)	Mean ice + snow thickness (m)	Chl <i>a</i> max depth (m)	Deployment position	Deploy time (hours)
19	28.05.15	81°17.4, 19°13.5	377	8	1.0	10	Ice edge	24
27	31.05.15	81°38.6, 17°58.6	876	9	1.5	40	Mid ice	24
31	03.06.15	81°62.0, 19°42.7	1963	10	1.4	10	Ice edge	24
32	06.06.15	81°23.3, 19°43.1	481	9	1.6	25	Mid ice	16
39	11.06.15	81°91.7, 13°45.9	1589	10	2.0	-	Mid ice	23
43	15.06.15	82°21.1, 7°58.8	804	10	1.3	-	Mid ice	24
46	17.06.15	81°89.1, 9°72.8	906	10	1.5	-	Mid ice	22
47	19.06.15	81°34.7, 13°60.9	2171	9	1.2	15	Mid ice	24

### 2.3 Water column sampling / Suspended profiles

Water samples were taken from 12-litre Niskin bottles mounted on a SBE32 Carousel Water Sampler with 24-bottles with the CTD/RO. Water samples (3 liters (L)) were collected from 8 depths between 10 and 200m for analysis of POC/PON, size-fractionated chlorophyll *a* and phaeopigments (total and >10 $\mu$ m), as well as nutrients (nitrate, nitrite, silicate and phosphate). Sample depths varied slightly depending on station, to get water from below, at and above the chlorophyll *a* maxima, based on the profile during downcast (table 2). At each station the CTD/RO profiler estimated the location of the chlorophyll *a* maximum using a fluorescence sensor during downcast, and Niskin bottles were fired accordingly on upcast. At station 19, located on the Barents Sea shelf break north of Svalbard (fig. 1), the bottom depth was assumed to be too shallow to sample at 200m.

For POC/PON, triplicates (300-500ml depending on concentration) were filtered onto a pre-combusted Whatmann GF/F filter and frozen at -20°C until later analysis in the lab at UiT in Tromsø. Chlorophyll *a* and phaeopigments triplicate samples (100-300ml) were filtered onto GF/F filters, as well as one 300ml sample filtered onto 10 $\mu$ m Millipore filters for the particles >10 $\mu$ m in size. These filters were also frozen at -20°C and stored for later analysis. Nutrient samples were collected in acid-washed 100ml plastic bottles, handled using clean Nitrile gloves, and immediately frozen at -20°C for later analysis at UiT. The respective analysis of the suspended profile samples is described in section 2.6.

Table 2. Sampled depths, in meters, for suspended vertical profiles of the eight sea ice stations, for chlorophyll *a* and phaeopigments, particulate organic carbon (POC) and nitrogen (PON), and nutrients. Chlorophyll *a* maximum shown, in meters, estimated by the CTD fluorescence sensor.

Station	Estimated depth of Chl <i>a</i> maximum (m)	Sampled depths (m)
19	20	10, 20, 30, 40, 50, 75, 100, 150
27	20	10, 20, 30, 40, 50, 75, 100, 200
31	25	10, 25, 30, 40, 50, 75, 100, 200
32	25	10, 25, 30, 40, 50, 75, 100, 200
39	35	10, 30, 35, 40, 50, 75, 100, 200
43	-	10, 20, 30, 40, 50, 75, 100, 200
46	-	10, 20, 30, 40, 50, 75, 100, 200
47	15	10, 15, 30, 40, 50, 75, 100, 200

## 2.4 Vertical export

Vertical export of organic material was studied in the upper 200m of the water column, as the sharpest decrease in vertical export is expected in the uppermost aphotic layer, and very little retention of organic material is evoked in waters deeper than 200m (Andreassen and Wassmann 1998, Boyd and Trull 2007, Renaud *et al.* 2008).

At each of the eight ice stations, one epipelagic array of sediment traps (fig. 2) was deployed at five depths (30, 40, 60, 90 and 200m) and recovered roughly 24 hours later. At station 19, the sediment trap array had to be restricted to 90m due to likelihood of drifting into shallow waters during the station time. The traps were deployed through drilled holes in the ice (1-2m thick), at a distance from the ship in order to avoid contamination and mixed surface waters due to the ship propellers. The sediment traps (KC Denmark AS) were a pair of transparent, parallel Plexiglas cylinders (7.2cm inner diameter and 45cm height; H:D ratio 6.25) mounted on a gimbaled frame. The frame allows the cylinders to

remain vertical and perpendicular to the current direction, even at moderate current velocities (Coppola *et al.* 2002). Since the traps were deployed for 24 hours, no fixatives or poisons were added to the cylinders upon deployment. The accuracy of these sediment traps have previously been confirmed in the Barents Sea, where  $^{234}\text{Th}$  data measured in suspended and trapped particles were used to measure their collection efficiency (Coppola *et al.* 2002, Lalande 2006). Upon retrieval, the traps were recovered by a winch, at a maximum speed of 0.5m/s to avoid turbulence and mixing in the cylinders. Once the traps surfaced, the contents of the two replicate trap cylinders were pooled (total 3.8L) into a clean plastic carboy, homogenized carefully and subsamples were collected for particulate organic carbon and nitrogen (POC, PON), size fractionated chlorophyll *a* and phaeopigment measurements (total and >10 $\mu\text{m}$ ), as well as for FP analysis. POC, PON, chlorophyll *a* and phaeopigments were filtered, following the same procedure as for the water column samples (section 2.4). Additional subsamples of 200ml were taken from each sediment trap depth and fixed with formaldehyde (2% final concentration) for FP investigations. All samples were stored cool and dark until analysis in the lab at UiT within a few months.

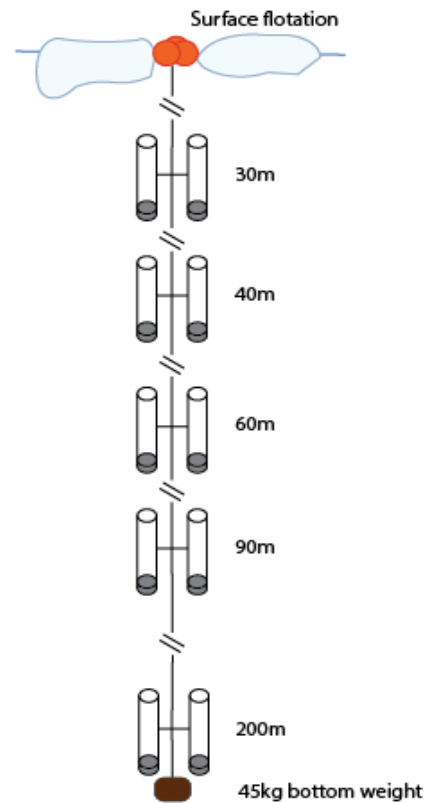


Figure 2. Sediment trap array, including surface floats for buoyancy and bottom weight of 45kg was attached. Deployment depths shown

## 2.5 Zooplankton FP production experiments

Incubation water (10L) for the FP production experiments was collected from depths close to the chlorophyll maxima at each of the stations, using the CTD Rosette. The water was carefully pre-screened through an 180µm mesh to remove larger grazers, and kept cold and dark prior to the experiments. Subsamples of the incubation water ( $T_0$ ) were taken during the experiment for later analysis, to correct for suspended FP introduced into the experiment via the incubation water. The  $T_0$  samples were filled along with the incubation chambers for the experiments, in a random rotating sequential manner, to ensure complete homogenization of the chambers and the  $T_0$  sample.

*Calanus* spp. for the FP production experiments were collected with vertical net tows from 100m depth using a WP-2 closing net (180µm mesh size) with a non-filtering cod-end (stations 19 and 27), and a Bongo net (500µm mesh size) (stations 31-47) (Table 3). The nets were towed vertically from 200m and 100m depths respectively, at low speeds. Immediately upon retrieval, zooplankton was gently transferred from the cod-end into a larger bucket filled with surface water, and transported into a cold and dark room.

Within 1 hour of the net tows, individual *Calanus* were sorted and selected for the experiments, with taxonomic identification following Kwasniewski *et al.* (2003) (described in further detail in section 2.8). The experiments were conducted on older, abundantly and dominant stages of *Calanus finmarchicus*, *Calanus glacialis* and/or *Calanus hyperboreus* (mostly CV stage or females) (table 3), as these were assumed to dominate in biomass and produce the largest proportion of FP in the water column (Arashkevich *et al.* 2002, Wexels Riser *et al.* 2008). Active individuals were gently picked out and kept in filtered seawater, on ice, until transferal into the experimental chambers, to ensure they were not feeding prior to the experiments. The health of each individual copepod was inspected prior to transferal. Depending on chamber condition (i.e. repairs needed) and incubation temperatures, between 5-7 replicate chambers, each containing 5 individual *Calanus*, were incubated. The chambers contained an inner suspended enclosure with a false bottom mesh (20µm), to prevent the copepods grazing on produced FP. The experimental chambers were incubated for approximately 6 hours in darkness. Prior to station 32, the chambers were incubated at a temperature of 4°C. Upon reflection and investigation of station water masses, a new incubation temperature of 0°C was chosen to reflect *in situ* temperatures (Wexels Riser *et al.* 2008). At stations 32-46 incubation temperatures of both 4°C and 0°C were chosen in order to investigate the within-station effect of temperature on FP production rate (table 3). At the end of each experiment, the contents of the experimental chambers were carefully sieved through a 10µm Nitex mesh, and the copepods and their FP were preserved with buffered

formalin (2% final concentration) for subsequent quantitative analysis (details in section 2.8.5).

Table 3. Summary of the fecal pellet (FP) production experiment, with the dominantly abundant *Calanus* species and stages incubated and the number of replicates performed, incubation start time in hours and temperature in °C, for each ice station for the chambers. The collection method of the *Calanus* in terms of net type and haul depth are also shown.

Station	<i>Calanus</i> Species / Life Stages Incubated (x #replicates)	Incubation time (hours)	Incubation Temperature	Net type and depth
19	<i>C. finmarchicus</i> F (x5)	6.50	5 chambers at 4°C	WP-2, 100m
27	<i>C. finmarchicus</i> (x3) <i>C. hyperboreus</i> F <i>C. hyperboreus</i> CV	6.25	5 chambers at 4°C	WP-2 100m
31	<i>C. hyperboreus</i> F (x3) <i>C. hyperboreus</i> CV <i>C. finmarchicus</i> F	6.25	5 chambers at 4°C	Bongo, 200m
32	<i>C. finmarchicus</i> (x3) <i>C. glacialis</i> F (x1) <i>C. hyperboreus</i> F (x1) <i>C. hyperboreus</i> CV (x2)	6.20	5 chambers at 4°C 2 chambers at 0°C	Bongo, 190m
39	<i>C. hyperboreus</i> F (x7)	6.00	4 chambers at 4°C 3 chambers at 0°C	Bongo, 200m
43	<i>C. hyperboreus</i> F (x6)	6.20	3 chambers at 4°C 3 chambers at 0°C	Bongo, 200m
46	<i>C. hyperboreus</i> F (x7)	6.00	4 chambers at 4°C 3 chambers at 0°C	Bongo 200m
47	<i>C. hyperboreus</i> F (x3) <i>C. finmarchicus</i> F (x3)	6.00	All chambers at 0°C	Bongo 200m

## 2.6 Laboratory analysis

### 2.6.1 Nutrients analysis

All nutrient samples from the suspended profiles were analyzed by standard seawater methods using a Flow Solution IV analyzer from O.I. Analytical, USA. The analyzer was calibrated using reference seawater from Ocean Scientific International Ltd., UK. The analysis and calibration was performed by Svein Kristiansen (AMB, UiT).

### 2.6.2 Chlorophyll *a* and phaeopigment analysis

Frozen GF/F filter samples, from both the suspended and exported profiles, were carefully placed into a glass tube, and the pigments were extracted overnight in methanol (5ml and 10ml respectively) at a temperature of 4°C. The samples were then homogenized using a



whirl and placed for analysis in a Turner Design AU-10 fluorometer. The fluorometer was initially calibrated with pure chlorophyll *a* (Sigma, C6144) (Holm-Hansen and Reimann 1978). Each filter sample was measured for chlorophyll *a*, and subsequently for the degradation product phaeopigment by the addition of two drops of hydrochloric acid (5% concentration). The measurement of phaeopigments was done to correct for the fact that phaeophytin *a* (phaeopigment) absorbs the same light wavelength and releases the same fluorescence as chlorophyll *a*, which can distort the true measure of the chlorophyll *a* in the cells (Rand *et al.* 1975).

The measure of chlorophyll *a* and phaeopigments was done following the equations:

$$\text{Chlorophyll } a \left( \frac{mg}{m^3} \right) = \text{Tau} * Fd * (Rb - Ra) * \frac{Vm}{Vs} \quad (1)$$

$$\text{Phaeopigments} \left( \frac{mg}{m^3} \right) = \text{Tau} * Fd * ((S * Ra) - Rb) * \frac{Vm}{Vs} \quad (2)$$

Where Tau is the correction factor between chlorophyll *a* and phaeophytin *a* (here found to be 2.02), and Fd is the calibration factor of the fluorometric reading against the concentration of pure chlorophyll *a* (here 1.566), found when the fluorometer was calibrated prior to the sample analysis. Rb is the fluorescence reading recorded prior to acid addition, and Ra is the fluorescence reading recorded after acid addition. Vm is the volume of methanol used for sample extraction (in ml), Vs is the volume of water filtered to obtain the sample (in ml), and S is an acid calibration factor (here 2.839).

### **2.6.3 Particulate organic carbon and nitrogen (POC, PON) analysis**

The frozen filter samples of POC/PON collected from the sediment traps and suspended profile were placed into glass tubes and covered with aluminum foil to avoid contamination. The samples were dried at 60°C for 24 hours. The samples then were placed in an acid fume bath (concentrated HCl) for 24 hours to remove all inorganic carbon on the filters. Subsequently the samples were replaced into the 60°C desiccator for an additional 24 hours. Once this preparation procedure was completed, the filter samples were “stuffed” into nickel capsules and stored in a vacuum exicator until analysis (within one month).

The samples were analyzed by an Exeter Analytical CE440 CHN elemental analyzer, which measures POC and PON through a series of combustive processes. The analyzer burns the filtered samples under static conditions in pure oxygen, at a temperature of 975°C, followed by a dynamic burst of oxygen. This results in the complete combustion of organics such as carbon and nitrogen into oxygenated gases, whilst removing inorganics and interfering gases such as halogens, sulfur and phosphorus. The gasses are then flushed with copper, which scrubs excess oxygen and reduce oxides of nitrogen into molecular nitrogen.

The gasses are then homogenized at constant pressure and temperature, and are passed through a series of high-pressure thermal conductivity detectors, each containing a pair of thermal conductivity cells. The first pair of cells is a water trap, which measures the amount of hydrogen in the sample, while the second pair is a carbon dioxide trap that allows for the determination of carbon. Finally, the remaining gas, nitrogen, is measured against a helium reference (used due to its stable nature in the columns). Blank samples were run at the beginning and end of each sample set (each containing 48 samples), and one pre-measured standard was run for every eighth sample. The blanks and standards (acetanilide) are measured and used as a reference for the measured filtered sample values, resulting in an output of hydrogen, carbon and nitrogen in the sample. Calculations done following:

$$\mu gC = \frac{R - Z - BC}{KC} - CFB \quad (3)$$

$$\mu gN = \frac{R - Z - BN}{KN} - NFB \quad (4)$$

Where R=signal value from sample ( $\mu V$ ), Z=blank value for helium gas ( $\mu V$ ), BC(BN)= blank carbon (and nitrogen) ( $\mu V$ ), KC(KN)=standard reference for carbon (and nitrogen), and CFB(NFB)=filter blanks for carbon (and nitrogen), which allow the machine to measure the relationship between carbon and nitrogen in the standard samples (in  $\mu g$ ).

The biomass of carbon and nitrogen could then be established for the suspended profiles, using the equation, here shown for carbon:

$$POC \left( \frac{mgC}{m^3} \right) = \frac{\mu gC}{Vf(l)} \quad (5)$$

Where Vf is the volume filtered, in liters.

## 2.7 Fecal pellet enumeration and measurements

To establish estimates of FP production and export rates, the 100ml samples from the FP production experiment, and 25-100ml subsamples from each of the sediment trap depths (volume depending on the concentration of pellets), were analyzed for FP material. Prior to analysis, the specific sample was thoroughly homogenized (20 careful rotations) and poured into an Utermöhl sedimentation column. The sample was subsequently left to sediment for roughly 24 hours prior to microscope enumeration.

Due to limited time for analysis, two sediment trap depths were chosen for FP analysis. The 40m sediment trap was chosen due to its placement just below the estimated chlorophyll *a* maximum (by the CTD/RO fluorometer) at all of the stations. The 90m-sediment trap was chosen as a comparison for flux regulation of FPC because, despite varied bottom

depth, 90m sediment traps have been previously found to accurately estimate export production to the sea floor and that weak retention happens below this depth (Renaud *et al.* 2008).

All the FP from the FP production experiment and the two sediment traps depths (40m and 90m) were counted and measured using an inverted microscope (100x magnification). The length and width of the FPs were measured in order to calculate FP volumes (FPV), using equation (9) (see section 2.8.5). The Leica inverted microscope used had a conversion factor of 0,00255mm per ocular unit.

Sizes of the individual *Calanus* copepods from the FP production experiments were measured using a Leica stereomicroscope, at 25x magnification. Prosome length was noted in mm, using the microscope conversion factor of 0.0025 mm per ocular unit (from calibration). During the copepod measurements, the sex and stages of the individual copepods were confirmed, following prosome length and urosome segments, as described by Kwasniewski *et al.* 2003. This paper was chosen for taxonomic separation of *Calanus* species because it followed the separation performed by Barbara Neihoff and Sandra Murawski (AWI) for the *Calanus* abundance data (see section 2.8.6).

## 2.8 Calculations

### 2.8.1 Sedimentation rates of chlorophyll a, POC and PON

In order to establish the daily flux of exported chlorophyll a, POC and PON, the sediment trap samples were converted from  $\text{mg m}^{-3}$  in the sediment traps to a daily export rate in  $\text{mg m}^{-2} \text{d}^{-1}$ , following the equation:

$$\text{Exported material (mg/m}^2\text{/d)} = \frac{\left[ X \left( \frac{\text{mg}}{\text{m}^3} \right) \right] * Vt}{At * d^{-1}} \quad (6)$$

Where X is the concentration of chlorophyll a, POC or PON measured from the filters sampled from the traps (in  $\text{mg m}^{-3}$ ), Vt is the volume of the sediment trap (in  $\text{m}^3$ ), At is the area of the sediment trap opening (in  $\text{m}^2$ ), and d is the sediment trap deployment time (in days).

### 2.8.2 Integrated suspended chlorophyll a and POC

To calculate the amount of chlorophyll a and POC material integrated in the upper 100m of the water column, the following equation was used:

$$\text{Integrated material } \left(\frac{\text{mg}}{\text{m}^2}\right) = \sum_{i=1}^8 \left( \frac{((sd_{i+1}) - sd_i)(X_i + (X_{i+1}))}{2} \right) \quad (7)$$

Where:

- $Sd_i$  = sampled depth  $i$  (e.g. 1=10m, 2=20m, 3=30m, 4=40m, 5=50m, 6=75m, 7=100m) (for other profiles, see table 2, section 2.4)
- $X_i$  = Chlorophyll a or POC concentration ( $\text{mg m}^{-3}$ ) at depth  $i$

### 2.8.3 Daily loss rate

Suspended biomass was integrated from 0-90m and was chosen to represent the total biomass available for vertical export. The upper 90m of the water column was investigated as attenuation is assumed to be weak below 90m depth, based on previous investigations in the northern Barents Sea and Arctic Basin (Olli *et al.* 2007, Renaud *et al.* 2008). Additionally, the deployment failure of the 200m depth sediment trap at station 19 made investigations into loss rates to 200m incomparable between all stations. Percent of daily biomass lost (%) to 90m was calculated by comparing this integrated suspended biomass to the export rates at 90m, following the equation:

$$\% \text{ Loss rate}_{90m} = \frac{\text{Export rate}_{90m} (\text{mg}/\text{m}^2/\text{d})}{\text{Integrated biomass}_{0-90m} (\text{mg}/\text{m}^2)} * 100 \quad (8)$$

Percentage loss was calculated for both POC and total chlorophyll a.

### 2.8.4 Estimate of Phytoplankton Carbon (PPC)

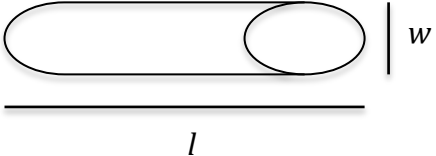
Primary production by phytoplankton produces organic compounds, especially carbon, from carbon dioxide. The amount of organic carbon produced by phytoplankton is not always directly proportional to chlorophyll a. In order to estimate the contribution of phytoplankton carbon (PPC) to exported POC, the relationship between all the POC and chlorophyll a measurements was investigated. The ratio between Chl a:POC reveals an estimate of the chlorophyll a to carbon correlation. Previous studies have found that Chl a:POC ratios are strongest during peak bloom development stages (Smetacek and Hendrikson 1979), as the contribution of chlorophyll a-rich phytoplankton will be greater than the contribution of deteriorating material, especially in the uppermost layers of the water column (M. Reigstad, *pers. comm.*). Therefore, the true chlorophyll a measurements found at each individual

station and depth, will be divided by an average Chl *a*:POC ratio between stations discovered to be peak bloom development, which are comparative to natural communities in the Barents Sea (Chl *a*:C of 0.031 (w:w) (Sakshaug *et al.* 2009)). This will yield an estimate of PPC, which will then be used to determine its relative contribution to POC flux (%PPC/POC exported).

### 2.8.5 Fecal pellet volume and sedimentation rates

In order to calculate sedimentation of FP collected by the sediment trap, the length and width of each pellet was converted into a fecal pellet volume (FPV).

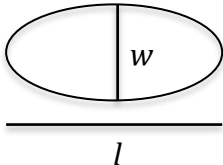
For copepod and krill FP, which generally have a cylindrical shape, FPV was estimated using the equation:



$$\text{Cylindrical FPV} = \pi * w^2 * \frac{l}{4} \quad (9)$$

Note that for both copepod and krill pellets length was measured from the ends of the longest segment of the pellet, and width was noted as the average width of the pellet measured. For copepod FPs, this may therefore have resulted in a minor underestimation of FPV, as they are elongated at the ends, making estimation of average width occasionally difficult.

For appendicularian FP, which generally have an ellipsoidal shape (Wilson *et al.* 2008; Miquel *et al.* 2015), FPV was estimated using the equation:



$$\text{Ellipsoid FPV} = \pi * l * \frac{w^2}{6} \quad (10)$$

The FPV equations use *l* as the length ( $\mu\text{m}$ ) and *w* as the diameter or width ( $\mu\text{m}$ ) of the FPs, giving FPV in  $\mu\text{m}^3$ . In order to obtain more manageable units, the FPV values were divided by  $1 \times 10^{-9}$ , to have FPV in  $\text{mm}^3$ . Stereometric conversions were done in accordance to Edler (1979).

According to values measured by Wexels Riser *et al.* (2007) in the northern Barents Sea, copepod FP generally contain  $94.5 \mu\text{gC mm}^{-3}$ , krill FP contain roughly  $45 \mu\text{gC mm}^{-3}$  and appendicularian FP were assumed to contain  $25 \mu\text{gC mm}^{-3}$ .

These carbon content values ( $\mu\text{gC mm}^{-3}$ ) were then multiplied by FPV ( $\text{mm}^3$ ), in order to acquire FPC ( $\mu\text{gC}$ ).

As with exported material from the sediment traps (chlorophyll and POC), the export rate of the pellets was found using the following formula:

$$FPC \text{ export rate} = \frac{FPC * Vf}{At * d^{-1}} \quad (11)$$

Where Vf is volume factor, At is area of the sediment trap opening and d is exposure time in days, following:

$$Vf = \frac{\text{total volume of trap}}{\text{volume analysed}} = \frac{1800ml}{50ml} \quad (12)$$

$$At = \text{Area of trap opening} = 4.07 * 10^{-3}m^2 \quad (13)$$

The result is a export rate of FPC in  $\mu\text{gC m}^{-2} \text{ d}^{-1}$ .

### 2.8.6 Community FPC production (0-40m)

*Calanus* copepod abundances from stations 19 and 31 were counted and provided by Barbara Neihoff and Sandra Murawski (AWI). Only two stations were investigated for community FPC production due to restricted time for analysis. The zooplankton samples were collected using multi-nets (0.25m<sup>2</sup> opening, 150 $\mu$ m mesh-size) from 50m depth. The abundances could be used to estimate the community production of FPs for the *Calanus* species and stages incubated for the FP production experiments (Table 2). The *Calanus* abundance count was given in mean number of individuals per cubic meter (ind m<sup>-3</sup>) and was integrated for the upper 40m of the water column. Community FPC production rates are estimated using the following equation:

$$\text{Community FPC prod.} \left( \frac{\text{mgC}}{\text{m}^2 \text{ d}} \right) = \text{Calanus}_{0-40m} \left( \frac{\text{ind}}{\text{m}^3} \right) * FPC \left( \frac{\text{mgC}}{\text{ind d}} \right) \quad (14)$$

For station 19, FP production was only examined for *C. finmarchicus* females, whilst station 31 was examined for *C. finmarchicus* females and *C. hyperboreus* females and CV. The FPC found in the 40m sediment trap was thoroughly examined and assumed *Calanus* FPs from the respective species were identified, and FPC was estimated (following equation 11, converted to mgC m<sup>-2</sup> d<sup>-1</sup>). This FPC rate was then used to estimate the proportion of community FPC production that was exported to 40m depth, using the equation:

$$\% \text{Community FPC export}_{40m} = \frac{\text{Calanus FPC export}_{40m} \left( \frac{\text{mgC}}{\text{m}^2 \text{ d}} \right)}{\text{Community FPC prod.} \left( \frac{\text{mgC}}{\text{m}^2 \text{ d}} \right)} * 100 \quad (15)$$

## **2.9 Statistical analysis**

The eight ice stations were investigated for the connectivity between the physical characteristics and the biology through a hierarchical cluster analysis (Greenacre and Primicerio 2013), using SYSTAT (Systat Software Inc., San Jose, CA, USA). A cluster analysis allows for visualization of connectivity of stations by grouping together those of closest similarity, and then merging them on dendrogram with a certain distance, giving the reader an impression of how closely linked some stations are to the rest. For the station data, a dendrogram using average linkage and Euclidean distance was done, joining temperatures, salinity, nutrient concentrations (nitrate, nitrite), chlorophyll *a* maxima depths, as well as suspended, exported and integrated chlorophyll *a*, phaeopigments, POC and PON concentrations, loss rates, percentage of large chlorophyll *a* cells (>10 $\mu$ m), FPC:POC ratios, and C:N ratios. Average linkage was used between the stations and their properties, which determines the distances between them. The Euclidean distance is a metric of dissimilarity of hierarchical clustering.

Statistical analysis was not performed on the FP production experiments, due to the limited sample size, which would have resulted in low power of the tests. Instead the results were visually inspected for variation between incubation temperature and species.

### 3. Results

#### 3.1 Physical characteristics of the sampling area

The eight stations investigated northwest of Svalbard (fig. 1) were found to vary greatly hydrographically. Stations 19 and 32, sampled 9 days apart (28<sup>th</sup> May and 6<sup>th</sup> June respectively), were located in close proximity on the shallower Barents Sea shelf break, around 20°E. These stations were characterized by cold water in the upper 30m, and with temperatures that increased rapidly down to 100m (fig. 3c). A steeper gradient in temperature and salinity was prominent at station 32, indicating a stratification layer with ArW in the upper 40m and AW under 75m ( $T > 2^{\circ}\text{C}$ ,  $S > 34.92$ ). Station 31, also located 20°E but further north and further into the AO basin, was found to have a very pronounced stratification layer between 25-40m (fig. 3b), with strong influence of the cold Arctic melt waters ( $T < -1.0^{\circ}\text{C}$ ,  $S < 34.5$ ) and an underlying layer of warmer and more saline AW ( $T > 2.0^{\circ}\text{C}$ ,  $S > 34.92$ ).

The stations located deeper off the Barents Sea shelf and into the Sofia deep (27, 31 and 47) revealed an interesting pattern in hydrography. A significant ArW influence ( $S < 34.2$ ) was discovered at the station deepest in the Sofia Basin (St. 47) down to 75m, but progressing further north-east (27 and subsequently to station 31), the influence of the ArW diminished whilst warmer and more saline AW was observed progressively shallower in the water column (fig. 3b) (Peeken 2016). This pattern coincides with the WSC (fig. 1), bringing AW around the coast of Svalbard and around the Yermak Plateau, being less prominent in the Sofia Basin (Soltwedel *et al.* 2000).

Stations 39, 43 and 46 on and around the Yermak Plateau were the stations located furthest north (fig. 1). These stations showed comparable temperature and salinity profiles, with the coldest ArW (roughly  $T = -1.8^{\circ}\text{C}$ ,  $S = 34.3$ ) down to 50m (fig. 3a). From 50-200m, no distinct AW was found ( $T < 2^{\circ}\text{C}$ ), indicating similar water masses originating in the area over the Yermak Plateau with less AW influence in the upper 200m. These stations showed no evidence of AW though the water column, with  $S < 34.92$  and  $T < 2^{\circ}\text{C}$  down to the bottom (appendix fig. A2).

The nitrogen nutrients available for new production (nitrate and nitrite) were reduced and low in the upper 30m of the water column at stations 19 and 32 ( $< 2.6 \text{ mmol m}^{-3}$ ), following their stratification layers. Low levels of surface nitrate and nitrite were also found at station 47 ( $1.65 \text{ mmol m}^{-3}$ ). In addition, stations 19, 32 and 47 had the lowest surface (10-30m) values for silicate ( $< 2.0 \text{ mmol m}^{-3}$ ) and phosphate ( $< 0.28 \text{ mmol m}^{-3}$ ) (data not shown). At the stations around the Yermak Plateau (39, 43, 46), nutrient concentrations were high and relatively homogenous with depth (fig. 3a).



All stations had extended sea ice cover (80-100%). Station 19 had the lowest cover of sea ice, while stations 31 and 39-47 had complete sea ice cover.

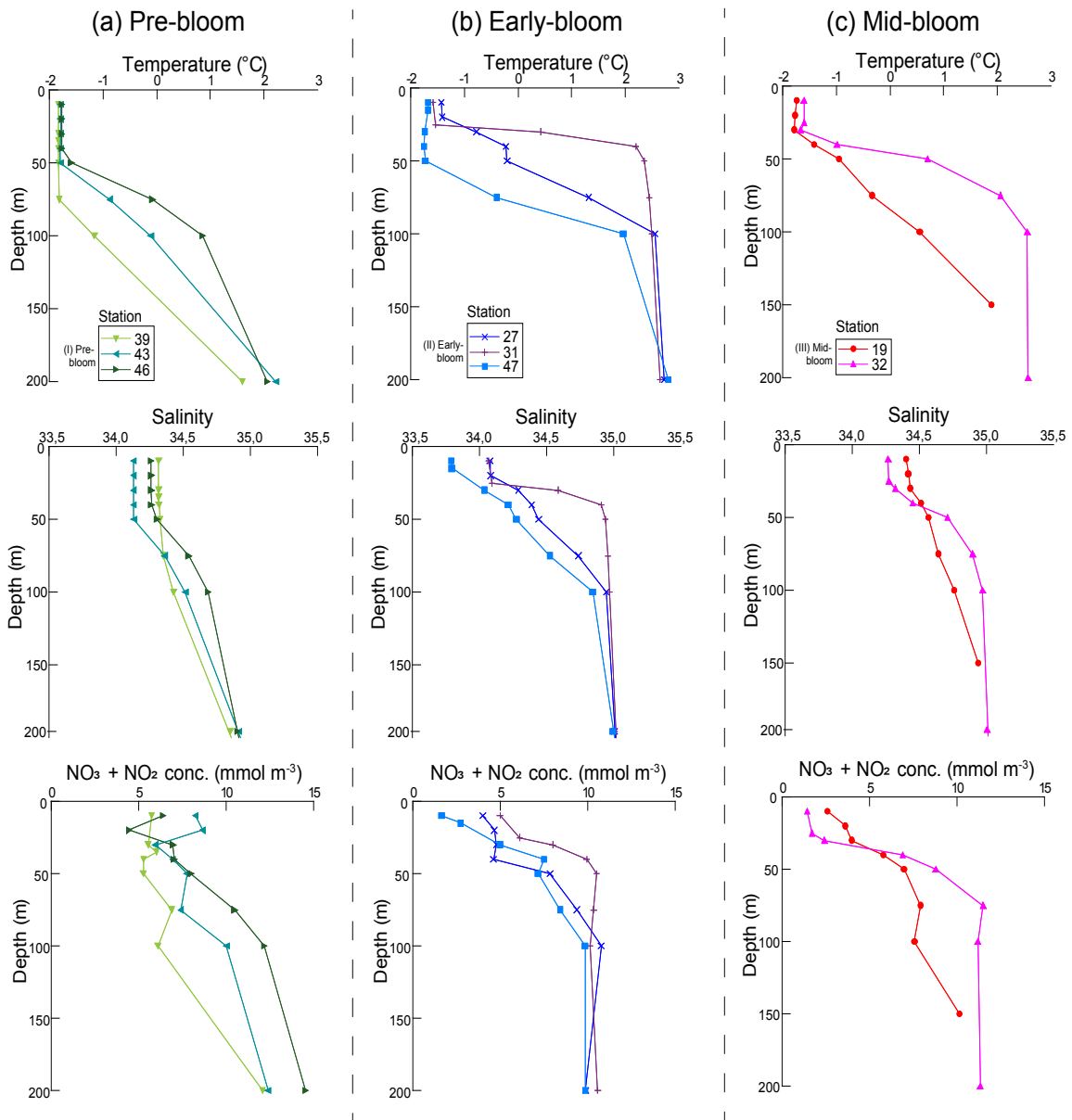


Figure 3. Temperature (°C) (upper), salinity (middle), and concentrations of nitrogen nutrients available for new production (mmol m<sup>-3</sup> of nitrate (NO<sub>3</sub>) and nitrite (NO<sub>2</sub>)) (lower) profiles for the eight sea ice stations. Stations grouped according to bloom development phase: (a) pre-bloom stations, (b) early-bloom stations, and (c) mid-bloom stations. Profiles are shown for the upper 200m, where suspended biological material was sampled.

### 3.2 Bloom development grouping

The stations were grouped according to bloom development, based on the hierarchical cluster analysis, comparing physical properties and the biology at each station. The analysis was used as a visual aid, where the cuts in clusters was made according to Euclidean

distances, as well as relative importance of key biological and biogeochemical characteristics (i.e. chlorophyll *a*, phaeopigment, POC and nitrate concentrations were given higher priority). Generally, the analysis revealed that the stations that were physically and biologically similar were stations 19 and 32 (group III); 27, 31 and 47 (group II); and 39, 43 and 46 (group I) (fig. 4, table 4). Stations 19 and 32 both had high levels of chlorophyll *a* and POC, suggesting that they were in a more developed stage of the bloom. Nutrients (nitrate, nitrite, silicate and phosphorus) were low but not depleted in the upper water column above the stratification layers (<30m) (fig. 3c, table 1), possibly indicating that they were not yet in a peak- or post-bloom state. Both stations were located in close proximity, but they were sampled 9 days apart, explaining the further depletion of surface nitrate and increase of chlorophyll *a* found at station 32. Group III stations were grouped as mid-bloom stations (table 3).

Stations 39, 43 and 46 (group I) were found closely associated, with very low levels of organic material in the water, as well as higher nutrient concentrations and similar temperature and salinity profiles (fig. 3a). They were grouped as pre-bloom stations (table 4).

Stations 31 and 47 were found clustered closely together. Station 27, despite being more dissimilar, was grouped with station 31 and 47, being in an intermediate stage of bloom development, where chlorophyll *a* and POC were progressively accumulating and phaeopigments still dominated over chlorophyll *a* (fig. 5b, appendix fig. A3). Since nitrate was not depleted in the upper water column at these stations (fig. 3b), it was supposed that they were in an early-stage of bloom development and were hence categorized as such (group II, table 4).

Additionally, the stations that were found to be fairly similar were located in relatively close proximity (fig. 1). Stations of group III were located on the Barents Sea shelf, group II were in the deeper Sofia Basin, and group I were located on or around the Yermak Plateau (fig. 1). Interestingly, group II stations could be considered in a similar bloom phase despite being sampled several weeks apart (table 1).

Table 4. Sea ice station groups, according to bloom development phase, showing average bottom depths, ice cover in the station areas, average depth of chlorophyll *a* maxima (m) according to suspended profile measurements, and the general geographical area in which the stations were located.

Group	Bloom development	Stations	Avg. bottom depth (m)	Ice cover (/10)	Avg. depth of Chl <i>a</i> max. (m)	Station region
I	Pre-bloom	39, 43, 46	1100	10	-	Yermak Plateau
II	Early-bloom	27, 31, 47	1670	9-10	20.0	Sofia Basin
III	Mid-bloom	19, 32	429	8-9	17.5	Barents Sea shelf break

## Hierarchical Cluster Tree

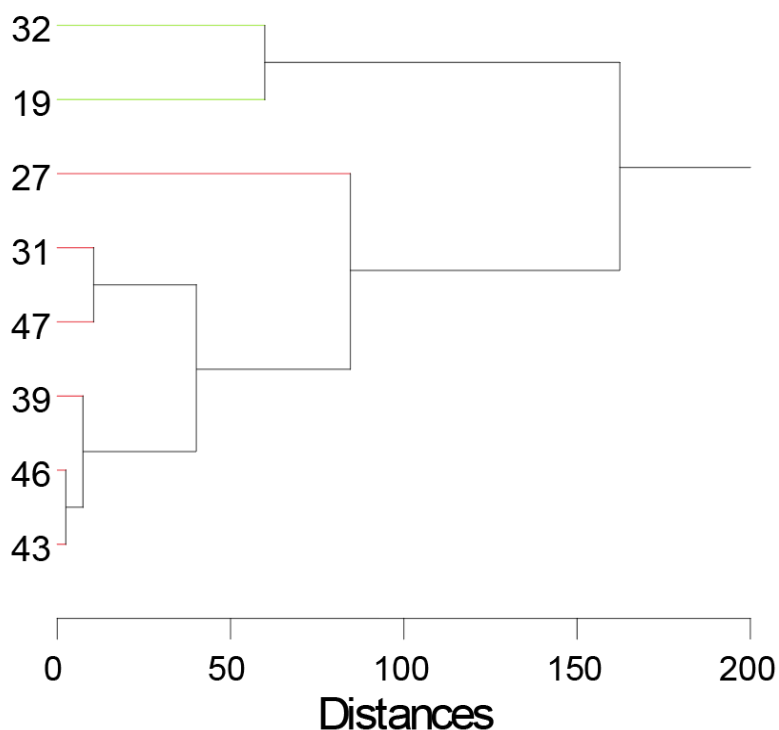


Figure 4. Hierarchical cluster analysis tree, indicating closeness of sea ice stations (left) in relation to station temperatures, salinity, nutrient concentrations (nitrate, nitrite), chlorophyll *a* maximum depths, as well as suspended, exported and integrated chlorophyll *a*, phaeopigments, POC and PON concentrations, loss rates, percentage contribution of large chlorophyll *a* cells (>10 $\mu$ m), and FPC:POC and C:N ratios. Euclidian distances (bottom) indicate dissimilarity index.

### 3.3 Suspended material

Vertical suspended biomass of chlorophyll *a* (total), POC and the POC:PON ratio for the upper 200m varied greatly between stations (fig. 5). Maximum chlorophyll *a* concentrations ranged from 0.3-0.4 mg m<sup>-3</sup> at the pre-bloom stations (group I) to 6.1-6.8 mg/m<sup>3</sup> at the mid-bloom stations (group III). The same trend was seen for POC, where the mid-bloom stations yielded over 6 times more POC at the maximum (317.6-390.6 mgC m<sup>-3</sup>) than the pre-bloom stations (48.4-60.7 mgC m<sup>-3</sup>). Early-bloom stations (group II) revealed intermediate concentrations for both chlorophyll *a* (1.3-3.0 mg m<sup>-3</sup>) and POC (139.1-229.1 mgC m<sup>-3</sup>) (fig. 5b). Most stations had the highest concentrations of chlorophyll *a*, POC and PON in the top 10-25m, then declining with depth, whilst station 31 had a slightly deeper maximum at 40m. Early-bloom stations had very low suspended material below 100m, whilst similar values were found below 150m depth at the mid-bloom stations. A strong correlation between POC and chlorophyll *a* concentrations was observed ( $R^2=0.92$ ,  $n=64$ ,  $y=49.7x+36.4$ )(appendix fig.

A4a), suggesting that most of the suspended POC in the water column derived from algal material. The low y-intercept of the regression likely indicates that a very low fraction of the POC is not of chlorophyll *a* origin.

POC:PON ratios varied between stations and no general trend with depth or bloom development was found (fig. 5). All stations had C:N ratio in the range of 5.7-6.7 at 10m. These values approximate the Redfield ratio (6.6), suggesting the source of carbon and nitrogen from algal biomass of low degradation. This C:N range generally persisted down to 75m depth at all stations. Stations 19 (mid-bloom) and 43 (pre-bloom) had a higher C:N ratio (10.8 and 9.7) at 150 and 100m, respectively.

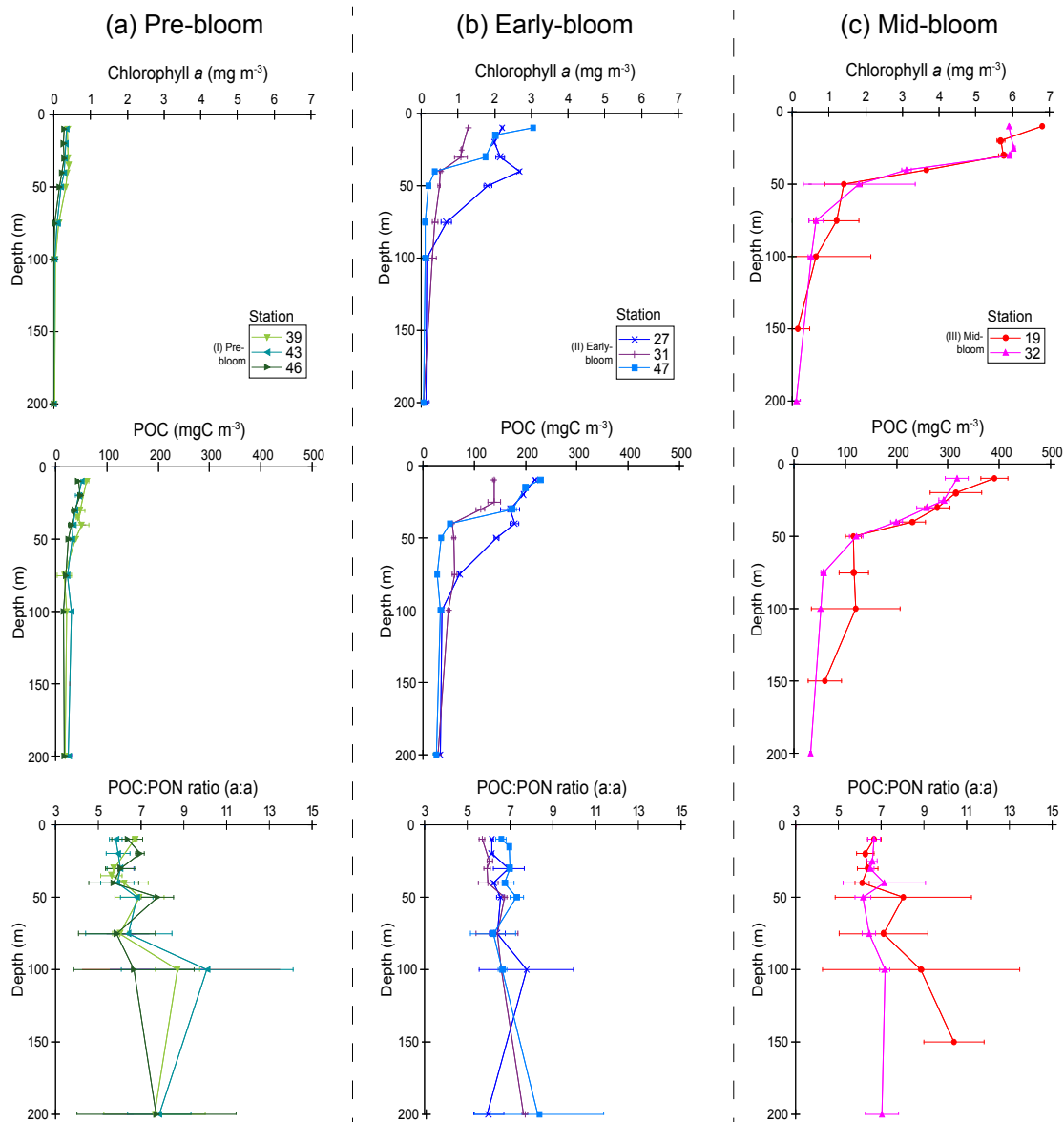


Figure 5. Vertical profiles of suspended chlorophyll *a* (upper) and particulate organic carbon (POC) (middle) concentrations in mg/m<sup>3</sup>, and POC:PON ratios (lower) in the upper 200m of each sea ice station. Stations grouped according to bloom development phase: (a) pre-bloom stations (group I), (b) early-bloom stations (group II), and (c) mid-bloom stations (group III). Average concentrations  $\pm$ SD ( $n=3$ ).

## 3.4 Vertical export

### 3.4.1 Daily chlorophyll *a* and phaeopigment flux

The material sampled by the sediment traps revealed similar trends in algal biomass as the vertical suspended profiles (fig. 6). Pre-bloom stations (group I) had very low export rates of chlorophyll *a* and phaeopigments, ranging from 0.1-0.4 mg m<sup>-2</sup> d<sup>-1</sup> at the maximum rates (fig. 6a). Mid-bloom stations (group III) had high export rates, peaking at 30m and declining with depth (fig. 6c). The maximum rate of chlorophyll *a* export was at station 32 (23.6 mg m<sup>-2</sup> d<sup>-1</sup>). Early-bloom stations (group II) had intermediate vertical export rates of phaeopigments and chlorophyll *a* (maximums ranging 0.8-6.5 mg m<sup>-2</sup> d<sup>-1</sup>), although no clear trend in the flux was found with depth (fig. 6b). Similarly to suspended algal material, station 31 had a deeper maximum of phaeopigment export (6.5 mg m<sup>-2</sup> d<sup>-1</sup>) at 90m.

The phaeopigment contribution to the exported material was larger than chlorophyll *a* at the early-bloom stations (fig. 6b), whilst the mid-bloom stations had considerably higher vertical fluxes of chlorophyll *a* (fig. 6c). At the pre-bloom stations, the vertical export rates of chlorophyll *a* and phaeopigments were comparable, although low (fig. 6a). Additionally, in the upper 40m of the water column at the mid-bloom stations, the contribution of phaeopigments was on average 54% lower than chlorophyll *a* (data not shown). This indicates that the least degraded algal flux occurs in the upper waters during mid-bloom development.

The contribution of large algal cells (>10µm) to the vertical export became more important with depth of the early-bloom stations (fig. 6b). This relationship was not consistent with the other station groups. Pre-bloom stations had the highest relative contributions of large cells to the fluxes in the upper sediment traps, and decreasing with depth (fig. 6a). At station 39 (pre-bloom), the contribution of large cells was very high in the 90m sediment trap (140%, result not plotted), indicating patchiness of large chlorophyll *a*-rich algal material at this station, possibly restrained to this discrete depth interval. The mid-bloom station 19 had the highest contribution of large cells (70-86%) to the vertical export. Comparable contributions were not discovered at the other mid-bloom station (32) (35-61%), where vertical chlorophyll *a* flux was highest (fig 6c).

For full overview of export rates, as well as phaeopigment and large cell contribution, see appendix (table A1).

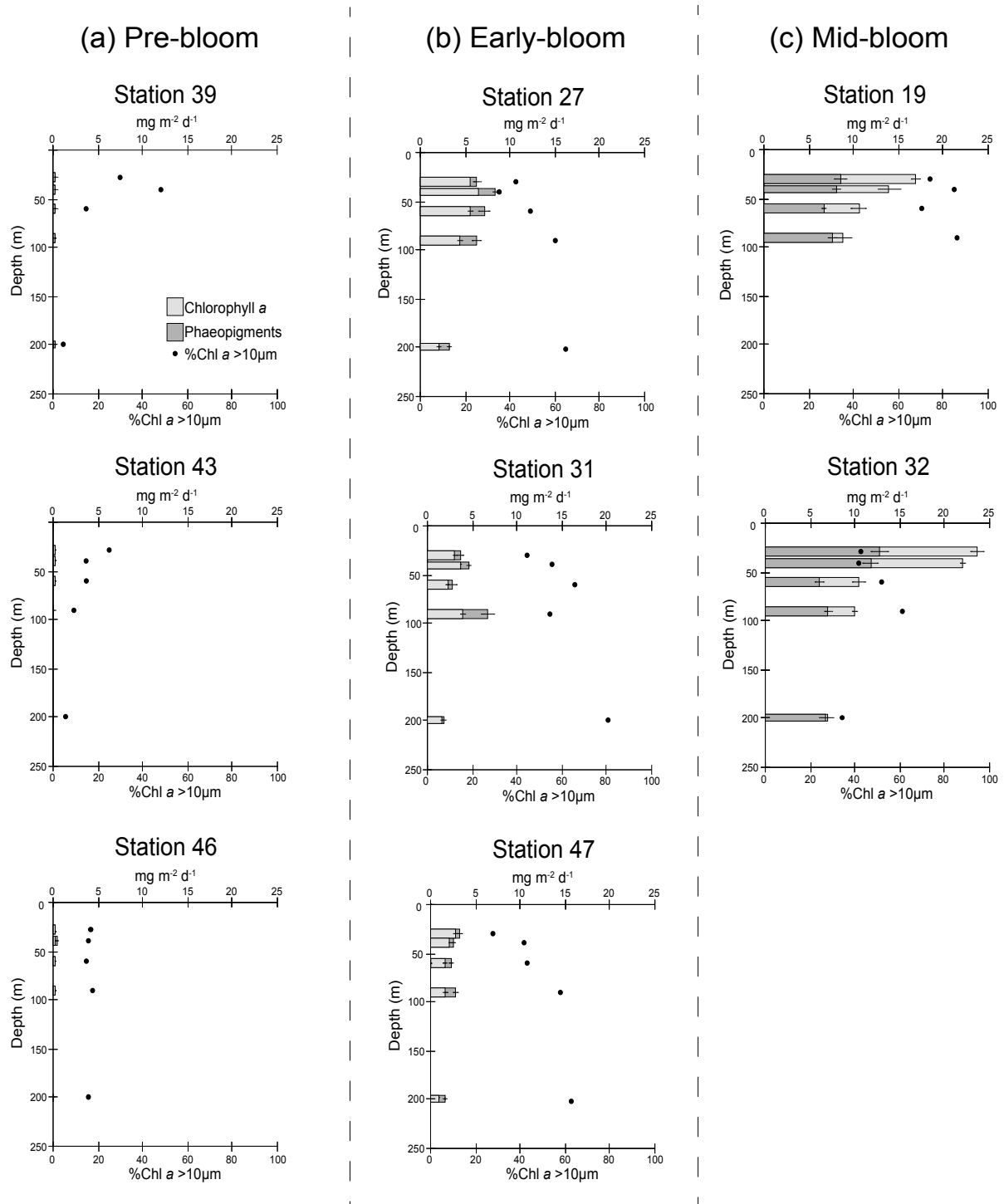


Figure 6. Vertical export rates of chlorophyll *a* and phaeopigments in  $\text{mg m}^{-2} \text{d}^{-1}$  (columns) for each of the deployed depth of the sediment traps, and the corresponding contribution of large chlorophyll *a* cells ( $>10\mu\text{m}$ ) in % (dots). Stations grouped according to bloom development phase: (a) pre-bloom stations (group I), (b) early-bloom stations (group II), and (c) mid-bloom stations (group III). Average export rates  $\pm\text{SD}$  ( $n=3$ ). Note that columns are not additive but overlap so that absolute value can be read by upper axis.

### **3.4.2 Daily POC flux and estimation of PPC contribution**

Highest daily flux of POC was found at the mid-bloom station, with maximum values at 30m (fig. 7c). Station 32 has the highest POC export rate of  $1164.6 \text{ mgC m}^{-2} \text{ d}^{-1}$ . POC:PON ratios were found slightly higher for the exported material than the suspended profiles (appendix). Pre-bloom stations had the lowest export rates of POC ( $26.7\text{-}102.9 \text{ mgC m}^{-2} \text{ d}^{-1}$ ) (fig. 7a), while early-bloom stations shows intermediate export rates ( $120.5\text{-}526.3 \text{ mgC m}^{-2} \text{ d}^{-1}$ ) (fig. 7b).

As with the suspended profile, a strong correlation between POC and chlorophyll *a* flux was found ( $R^2=0.98$ ,  $n=39$ ,  $y=48.9x+62.0$ )(appendix fig. A4b), with a low y-axis intercept, suggesting most of exported POC was derived from algal material. In order to examine this further, contribution of PPC was estimated (fig. 7), using the average Chl *a*:POC ratios from the upper waters (30-40m) of the mid-bloom stations, where the contribution of degraded algal material was the lowest (roughly 50%) and the correlation between chlorophyll *a* and POC was the strongest (Chl *a*:POC of 0.027 (w:w),  $R^2=0.998$   $n=4$ , for the exported material). Bloom phase related increase in PPC contribution was found, with %PPC/POC averaging from 13% at pre-bloom stations, 45% at early-bloom stations, and 71% at mid-bloom stations (table 5). The largest relative contribution of PPC was found at station 32 (72-75%), and the lowest at station 39 (5-16%). Early-bloom stations showed the greatest variation in PPC contribution with depth (fig. 7b) and all had a peak PPC in contribution at 90m, whilst at the pre-bloom and mid-bloom stations it remained relatively constant (fig. 7a and 7c respectively).

POC:PON ratios were very similar to the suspended profiles although slightly higher (average 8.1 at 30m depth, appendix fig. A5). Highest C:N ratio discovered at station 43 (pre-bloom) of 11.0 at 90m depth, suggesting that some of the organic material in the water was degraded. On average, the mid-bloom stations had the highest C:N ratio (of 8.8 (a:a)) and the early- and pre-bloom stations had slightly lower ratios (7.5 and 7.7 respectively (table 5). This can indicate that as the bloom progressed, the organic material exported becomes slightly more degraded.

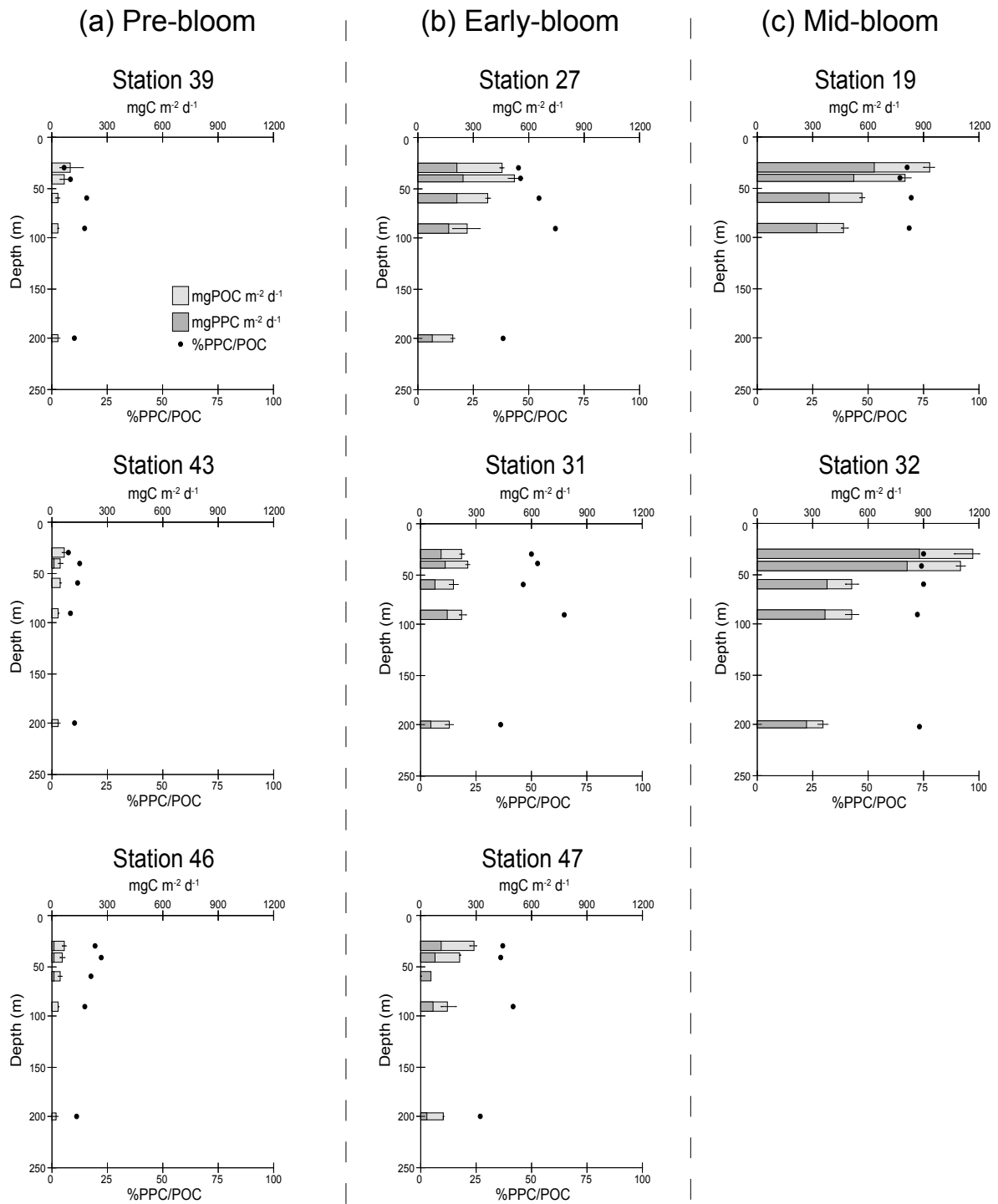


Figure 7. Vertical export rates of particulate organic carbon (POC) and estimation of export rates of phytoplankton carbon (PPC) in  $\text{mgC m}^{-2} \text{d}^{-1}$  (columns), and relative contribution of PPC to the POC flux (dots, in %) at each sediment trap depth. Stations grouped according to bloom development phase: (a) pre-bloom stations (group I), (b) early-bloom stations (group II), and (c) mid-bloom stations (group III). Average POC export rates  $\pm$ SD ( $n=3$ ). Note that columns are not additive but overlap so that absolute value can be read by upper axis.



### 3.5 Integrated profiles and biomass lost to 90m depth

#### 3.5.1 Integrated biomass and contribution of large cells

Integrated chlorophyll *a* and POC biomass for the vertical profile 0-90m varied greatly between stations (fig. 8, fig. 9a). The integrated biomass was lowest at the pre-bloom stations around the Yermak Plateau, ranging from 15.2-28.6 mg m<sup>-2</sup>, and highest at the mid-bloom stations on the Barents Sea shelf break, with a maximum found at station 19 (331.8 mg m<sup>-2</sup>). The integrated contribution of large cells (>10µm) showed a similar trend (fig. 8). Pre-bloom stations had a low proportion of large cells (6-8%), while mid-bloom stations had the highest (85-86%). Notably, station 31 had a high contribution of large cells (71%) despite having a significantly smaller chlorophyll *a* biomass (83.8 mg m<sup>-2</sup>).

Integrated POC standing stock (0-90m) also increased considerably from pre-bloom to mid-bloom stations, ranging from 3.8-23.6 gC m<sup>-2</sup> (fig. 9a).

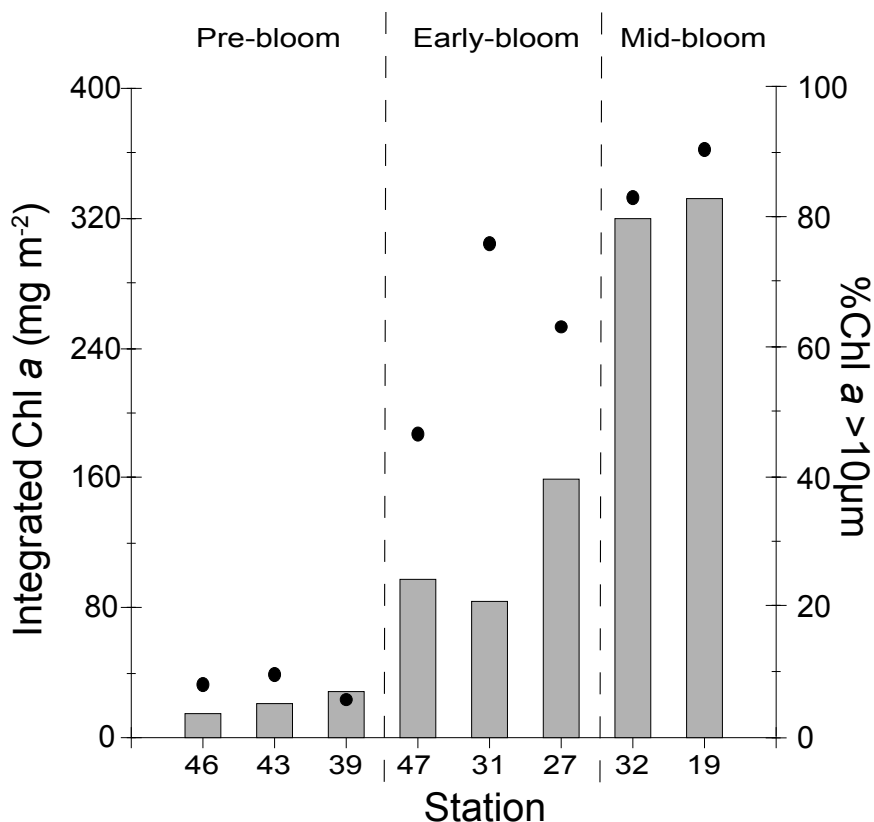


Figure 8. Integrated chlorophyll *a* in mg m<sup>-2</sup> (columns) and the corresponding contribution of large cells in % (dots). Chlorophyll *a* and its large fraction were integrated from the suspended standing stock (0-90m).

### 3.5.2 Daily loss rates to 90m depth

The daily proportion of POC loss (90m) was low for all stations but generally increased from pre to mid-bloom stations, ranging 0.6-2.7% (3-fold increase) (table 5, fig. 9a). The proportion of chlorophyll *a* standing stock lost (90m) showed a similar increase from pre to mid-bloom stations, ranging 0.3-3.1% per day (table 5), although station 31 (early-bloom) had a significantly higher daily loss rate (4.7%) than any other stations (fig. 9b). This is due to high flux of chlorophyll *a* to 90m, despite low general standing stock in the water column above (0-90m).

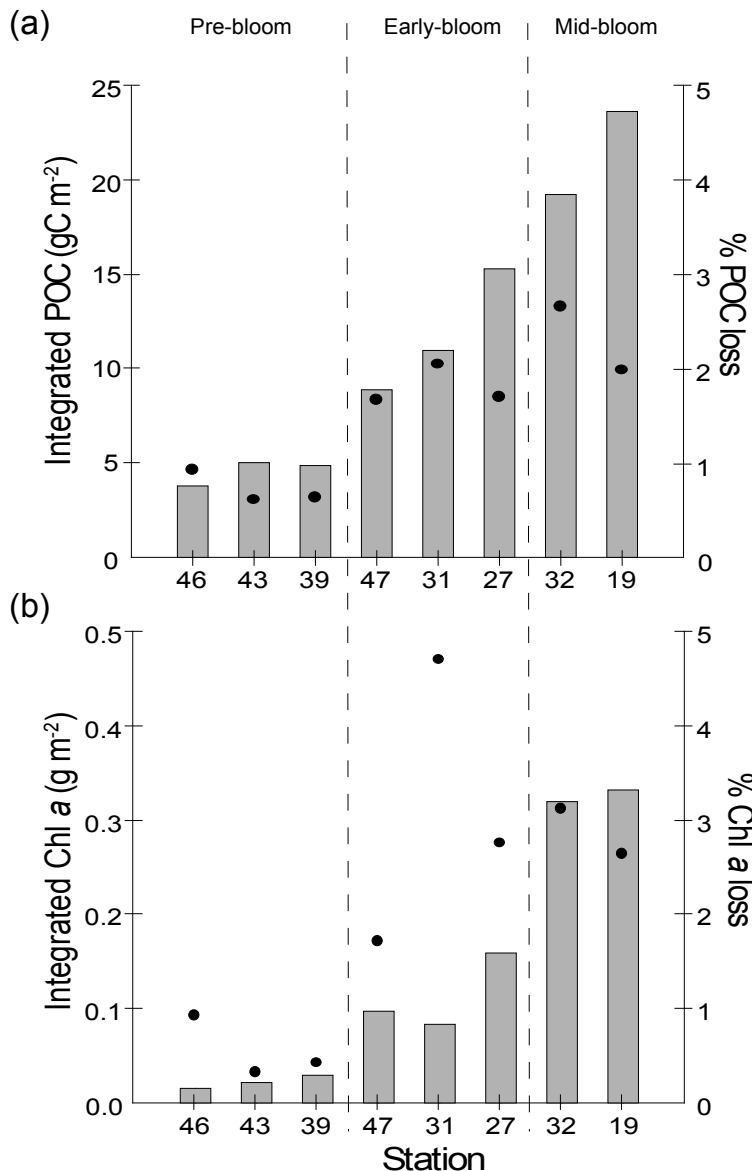


Figure 9. Integrated (a) particulate organic carbon (POC) and (b) chlorophyll *a* in g m<sup>-2</sup> (columns), and the corresponding percentage daily loss rates (dots). POC and chlorophyll *a* was integrated from the suspended standing stock (0-90m). Percentage loss is the proportion of the POC and chlorophyll *a* integrated biomass lost through vertical flux to the 90m sediment trap depth. Stations are grouped according to their bloom development phase. Note difference in scale.

Table 5. A summary of station characteristics, categorized according to bloom development phase, with average exported POC:PON ratios, and average % daily loss rate of particulate organic carbon (POC) and chlorophyll *a* (0-90m), in % per day. All values are averages from exported (sediment trap) samples, and the range within the grouped stations is shown in parentheses.

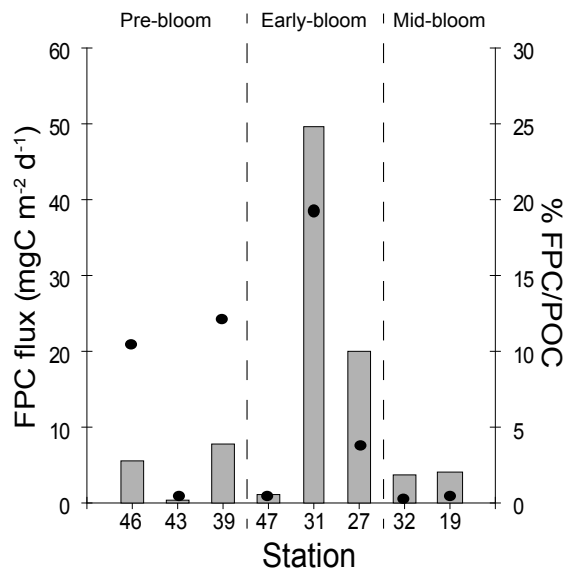
Group	Scenario	Stations	Exported C:N ratio (a:a)	Daily POC loss (%)	Daily Chl <i>a</i> loss (%)
I	Pre-bloom	39, 43, 46	8.8 (7.8-9.6)	0.7 (0.6-0.9)	0.6 (0.3-0.9)
II	Early-bloom	27, 31, 47	7.5 (7.2-8.0)	1.8 (1.7-2.1)	3.1 (1.7-4.7)
III	Mid-bloom	19, 32	7.7 (7.4-8.0)	2.3 (2.0-2.7)	2.9 (2.6-3.1)

### 3.6 Daily FPC flux

The early-bloom stations 27 and 31 revealed little variation in FPC flux between 40 and 90m (fig. 10), indicating that little retention of FP occurred in the water between 40 and 90m. The pre-bloom stations revealed a decrease in FPC flux from 40 to 90m (on average varying from 4.5 to 0.3 mgFPC m<sup>-2</sup> d<sup>-1</sup>), whilst the mid-bloom stations revealed an increase in FPC flux from 40 to 90m (on average varying from 3.9 to 21.4 mgFPC m<sup>-2</sup> d<sup>-1</sup>), possibly indicating higher production of FP below 40m (i.e. grazers are located below 40m in the water column). The highest FPC flux rates at 90m were found at the early-bloom stations (29.6-53.8 mgC m<sup>-2</sup> d<sup>-1</sup>), and lowest at the pre-bloom stations (0.0-0.9 mgC m<sup>-2</sup> d<sup>-1</sup>) (fig. 10b).

The contribution of FPC to the total POC flux also varied greatly between stations and bloom phases (fig. 10). The lowest overall contribution of FPC to POC flux (over both 40m and 90m) was at the mid-bloom stations, ranging from 0.3-0.5% at 40m and 2.8-6.0% at 90m. Highest contributions were discovered at early-bloom stations (ranging 0.5-23.9%). Average %FPC/POC for all stations and depths was 7.4%.

(a) 40m



(b) 90m

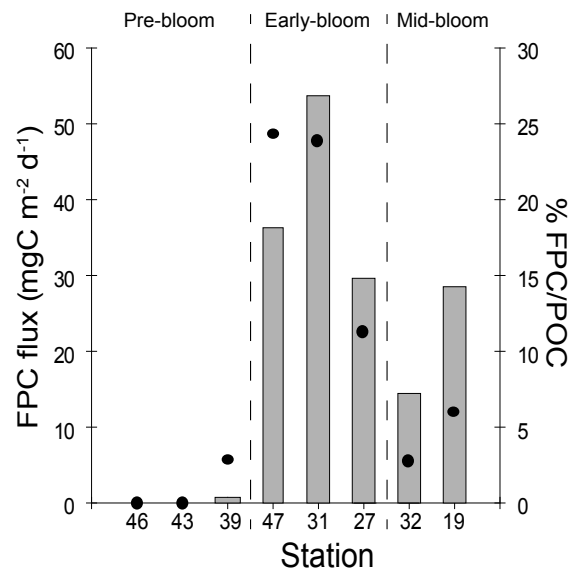


Figure 10. Vertical export rates of cumulative fecal pellet carbon (FPC) in  $\text{mgFPC m}^{-2} \text{d}^{-1}$  (columns) and the respective percentage FPC contribution of total particulate organic carbon (POC) flux (dots) at the 8 ice stations measured at: (a) 40m and (b) 90m depth. Stations grouped according to bloom development phase.

Furthermore, the distinctively largest difference in export of FPC from 40-90m was found at station 47 (early-bloom phase), where FPC flux increased from  $1.1\text{-}36.5 \text{ mgFPC m}^{-2} \text{d}^{-1}$ . The contribution of FPC flux to total POC flux was also the highest at this station at 90m (24%) (fig. 10b). This indicates that this station, despite lower POC standing stock, had proportionally higher amounts of FP sinking to 90m. The largest contribution of sinking FP was found to be most likely from copepods (fig. 11b).

Most of the stations had FPC flux likely derived from copepod FPs (fig. 11), although station 19 (mid-bloom) had mostly krill-like FPC at 90m (fig. 11b). Krill FPC was also found at stations 27 and 39 at 40m, and 19, 27, 31, and 32 at 90m. Notably, krill FPC flux at 90m was important only at the stations in the eastern section of the study area, over the shelf break of the northern Barents Sea. Appendicularian pellets were present at early-bloom stations and station 32 at 40m (fig. 11a), and only at station 47 in the Sofia basin at 90m (fig. 11b).

No correlation was found between FPC flux and POC flux ( $R^2 < 0.0005$ ,  $n=16$ ), nor between the FPC flux to 90m and the integrated chlorophyll *a* biomass (0-90m) ( $R^2=0.074$ ,  $n=8$ ). Furthermore, very weak correlations were found between FPC flux and chlorophyll *a* or phaeopigments ( $R^2=0.13$ ,  $n=16$ ), indicating no clear relationship between exported FP material and food available for the grazers.

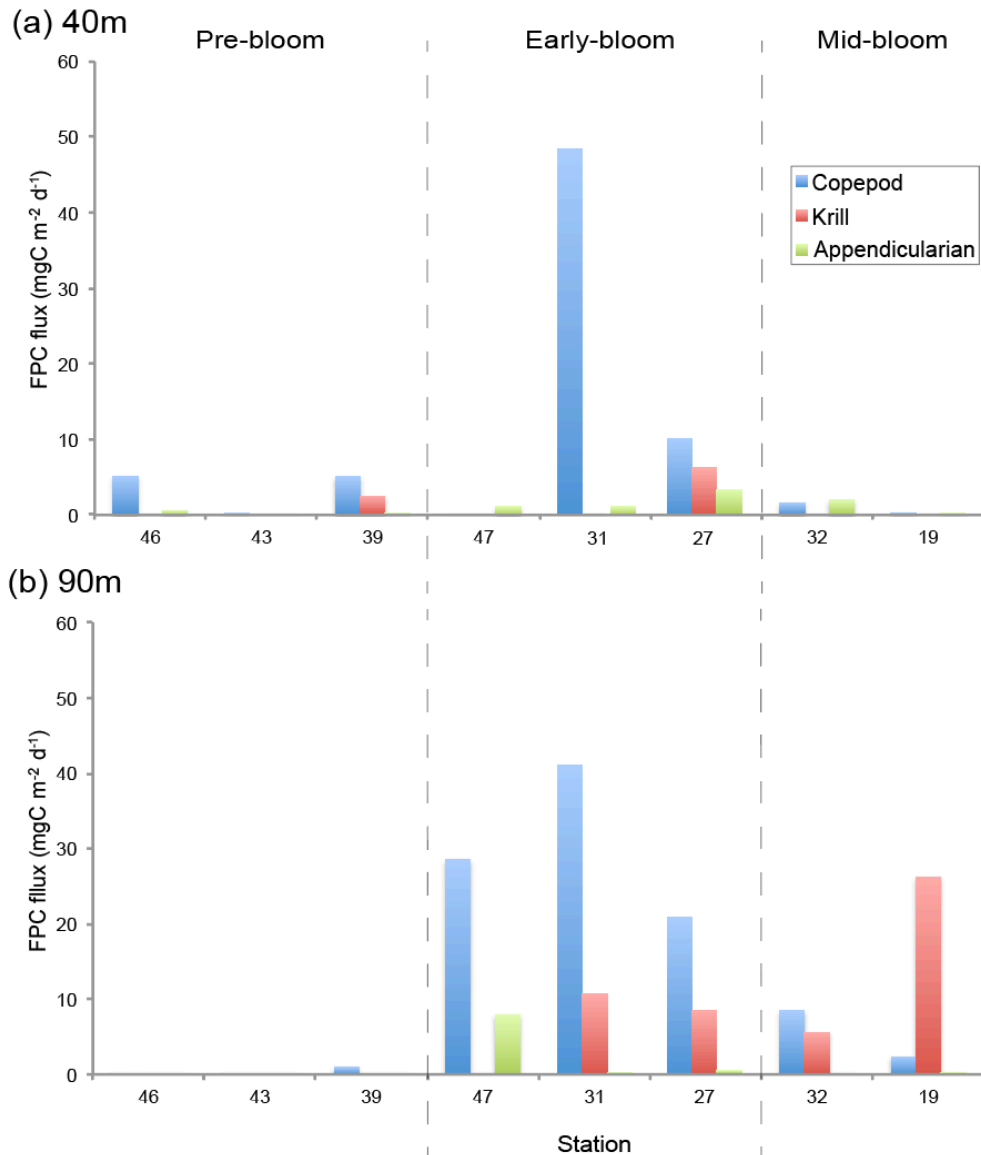


Figure 11. Vertical export rates of fecal pellet carbon (FPC) in  $\text{mgC m}^{-2} \text{d}^{-1}$  (columns) with likely FP origin split into copepod (blue columns), krill (red columns) and appendicularian (green columns). FPC rates are shown for export to the (a) 40m and (b) 90m sediment traps.

### 3.7 FP production and community grazing

#### 3.7.1 FP production

FP production rates varied greatly between the stations (fig. 12). The average production rate for the pre-bloom stations, dominated by *C. hyperboreus*, was  $0.37 \mu\text{gFPC ind}^{-1} \text{d}^{-1}$  (fig. 12a), producing 0.06 FP per individual per hour (fig. 12b). The early-bloom stations, where both *C. hyperboreus* and *C. finmarchicus* were abundant, *C. hyperboreus* produced an average of  $22.30 \mu\text{gFPC ind}^{-1} \text{d}^{-1}$  (fig. 12a) with  $1.05 \text{FP ind}^{-1} \text{h}^{-1}$  (fig. 12b), whilst *C. finmarchicus* averaged  $5.37 \mu\text{gFPC ind}^{-1} \text{d}^{-1}$  (fig. 12a), with  $1.23 \text{FP ind}^{-1} \text{h}^{-1}$  (fig. 12b). Finally, mid-bloom stations of the Barents Sea shelf break where mostly *C. finmarchicus* females (F)

were dominant, found the average production to be  $17.67 \mu\text{gFPC ind}^{-1} \text{d}^{-1}$  (fig. 12a), with  $3.22 \text{ FP ind}^{-1} \text{h}^{-1}$  (fig. 12b). Mid-bloom station 32 found *C. hyperboreus* females producing  $22.31 \mu\text{gFPC ind}^{-1} \text{d}^{-1}$  (fig. 12a), at an average rate of  $1.03 \text{ FP ind}^{-1} \text{h}^{-1}$  (fig. 12b).

The experiment revealed that generally, the number of FP produced by copepods per hour increases as chlorophyll *a* concentration increases (fig. 12). *C. finmarchicus* was found to produce the greatest number of pellets per hour (fig. 12b), with a maximum at the mid-bloom stations ( $2.11 \text{ FP ind}^{-1} \text{h}^{-1}$  at station 19), but being small in size, they contained lower amounts of FPC. Large *C. hyperboreus* females were found to produce the most FPC at the early-bloom stations and mid-bloom station 32, with a maximum of  $48.01 \mu\text{gFPC ind}^{-1} \text{d}^{-1}$  at station 27 (although this was only from one chamber, hence potentially biased). No strong correlations were found between the suspended chlorophyll *a* concentrations and the FPC production and number of FP produced by *C. hyperboreus* at the relevant stations ( $R^2=0.067$  and  $0.165$  respectively,  $n=13$ ). Table 6 gives a full summary of the FP production experiment and associated chlorophyll *a* concentrations and incubation temperatures.

Due to low sampling size, statistical analysis was not performed on the experimental data. Through observation of the data it could be suggested that the larger copepods (prosome length, table 6), especially *C. hyperboreus* females, produce the largest most carbon-rich pellets. No effect of incubation temperature or life stage on production rates could be discerned due to the lack of sufficient number of comparable replicates.

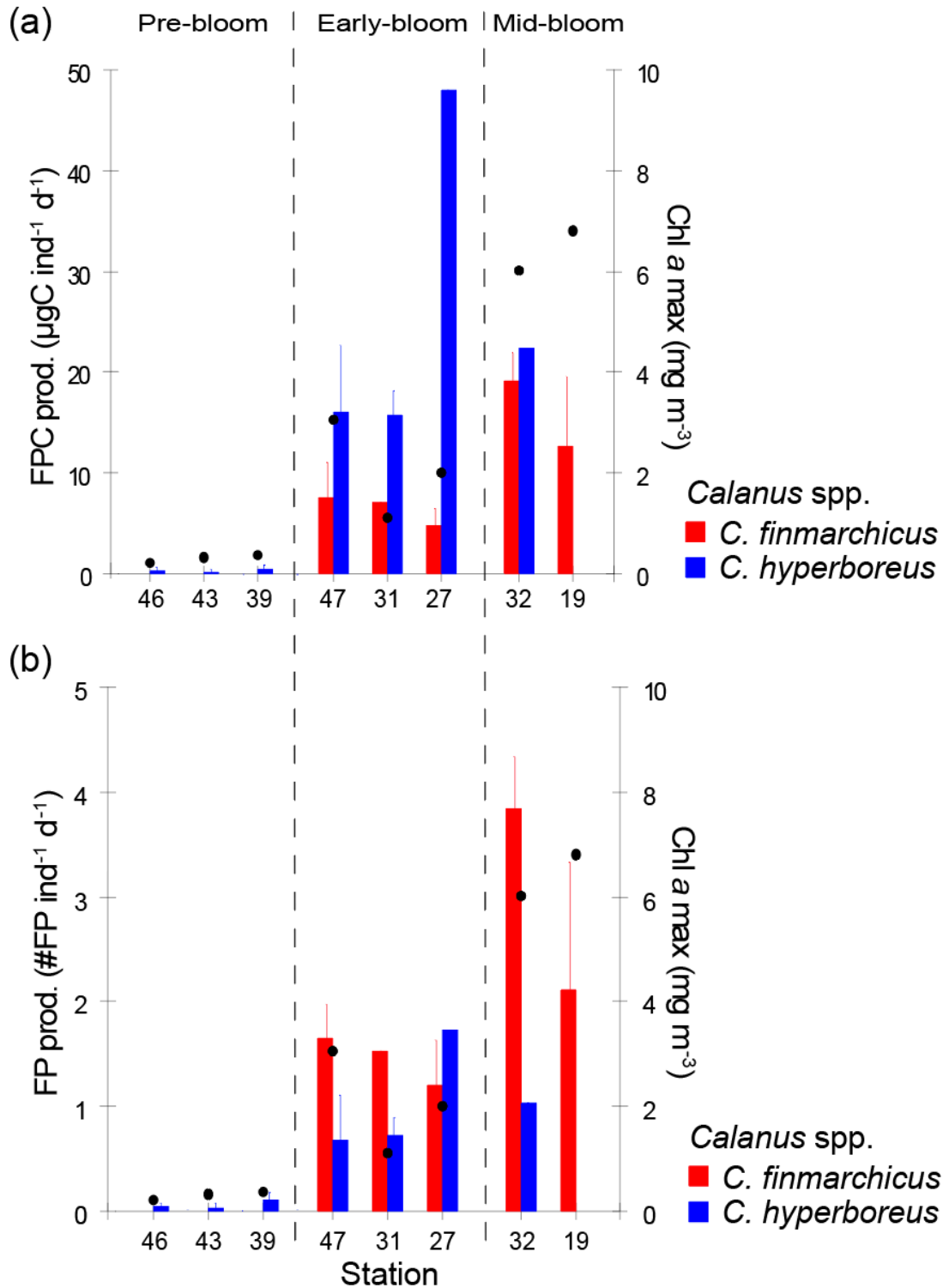


Figure 12. Fecal pellet (FP) production rates and chlorophyll a concentrations assumed for the incubation water, in  $\text{mg m}^{-3}$ , as the maximum values of the suspended vertical profiles at the respective stations. (a) Rate of fecal pellet carbon (FPC) production in  $\mu\text{gC ind}^{-1} \text{d}^{-1}$ , and (b) rate of FP production in number of FP produced per individual copepod per hour ( $\#\text{FP ind}^{-1} \text{h}^{-1}$ ). FP production rates separated for dominant *Calanus* copepod species incubated: *C. finmarchicus* females (red columns) and *C. hyperboreus* females (blue columns). Stations grouped according to bloom development phase. Standard deviations between replicates are given ( $n=2-5$ , table 6). Note difference in scale.

Table 6. FP production rates in  $\mu\text{gC ind}^{-1} \text{d}^{-1}$  and in  $\#\text{FP ind}^{-1} \text{h}^{-1}$ , for the respective stations and *Calanus* spp. incubated during the experiment. Average prosome lengths used for taxonomic identification of species and life stage shown in  $\text{mm} \pm\text{SD}$  ( $n=2-5$ ). Chlorophyll *a* concentrations (in  $\text{mg m}^{-3}$ ) for the incubations are estimations based on the average suspended concentrations from the chlorophyll *a* maxima  $\pm\text{SD}$  ( $n=3$ ). Average FP production rates are shown when replicates of the same spp. and stage were investigated  $\pm\text{SD}$  ( $n=2-5$ ).

Station	<i>Calanus</i> spp. / life-stages incubated (x replicates)	Incubation temp. ( $^{\circ}\text{C}$ )	Avg. prosome length (mm) ( $\pm\text{SD}$ )	FPC prod. ( $\mu\text{gC ind}^{-1} \text{d}^{-1}$ ) ( $\pm\text{SD}$ )	FP prod. (FP $\text{ind}^{-1} \text{h}^{-1}$ ) ( $\pm\text{SD}$ )	Chl <i>a</i> ( $\text{mg m}^{-3}$ ) ( $\pm\text{SD}$ )
19	<i>C. finmarchicus</i> F (x5)	4	2.87 ( $\pm 0.26$ )	12.66 ( $\pm 6.92$ )	2.11 ( $\pm 1.23$ )	6.80 ( $\pm 0.03$ )
27	<i>C. finmarchicus</i> F (x3)	4	2.87 ( $\pm 0.18$ )	4.85 ( $\pm 1.64$ )	1.20 ( $\pm 0.44$ )	2.00
	<i>C. finmarchicus</i> CV (x1)	4	2.89 ( $\pm 0.40$ )	1.88	0.53	( $\pm 0.03$ )
	<i>C. hyperboreus</i> F (x1)	4	6.36 ( $\pm 0.68$ )	48.01	1.73	
31	<i>C. hyperboreus</i> F (x3)	4	6.67 ( $\pm 0.45$ )	15.76 ( $\pm 2.46$ )	0.73 ( $\pm 0.16$ )	1.11
	<i>C. hyperboreus</i> CV (x1)	4	4.38 ( $\pm 0.91$ )	9.44	1.04	( $\pm 0.02$ )
	<i>C. finmarchicus</i> F (x1)	4	3.06 ( $\pm 0.06$ )	7.10	1.52	
32	<i>C. glacialis</i> F (x1)	4	3.59 ( $\pm 0.20$ )	6.58	1.69	6.02
	<i>C. finmarchicus</i> F (x2)	4	3.02 ( $\pm 0.13$ )	19.16 ( $\pm 2.79$ )	3.96 ( $\pm 0.63$ )	( $\pm 0.05$ )
	<i>C. finmarchicus</i> F (x1)	0	2.78 ( $\pm 0.16$ )	21.19	3.60	
	<i>C. hyperboreus</i> F (x1)	4	6.83 ( $\pm 0.19$ )	22.31	1.03	
	<i>C. hyperboreus</i> CV (x1)	4	5.27 ( $\pm 0.28$ )	6.84	0.84	
	<i>C. hyperboreus</i> CV (x1)	0	3.71 ( $\pm 0.08$ )	1.52	0.21	
39	<i>C. hyperboreus</i> F (x4)	4	6.82 ( $\pm 0.28$ )	0.39 ( $\pm 0.46$ )	0.07 ( $\pm 0.09$ )	0.37
	<i>C. hyperboreus</i> F (x3)	0	6.73 ( $\pm 0.23$ )	0.87 ( $\pm 0.41$ )	0.13 ( $\pm 0.05$ )	( $\pm 0.01$ )
43	<i>C. hyperboreus</i> F (x3)	4	6.79 ( $\pm 0.26$ )	0.20 ( $\pm 0.20$ )	0.05 ( $\pm 0.04$ )	0.33
	<i>C. hyperboreus</i> F (x3)	0	6.46 ( $\pm 0.37$ )	0.03 ( $\pm 0.06$ )	0.01 ( $\pm 0.01$ )	( $\pm 0.00$ )
46	<i>C. hyperboreus</i> F (x4)	4	6.76 ( $\pm 0.32$ )	0.38 ( $\pm 0.26$ )	0.03 ( $\pm 0.04$ )	0.22
	<i>C. hyperboreus</i> F (x3)	0	6.76 ( $\pm 0.32$ )	0.34 ( $\pm 0.22$ )	0.04 ( $\pm 0.01$ )	( $\pm 0.01$ )
47	<i>C. hyperboreus</i> F (x3)	0	6.81 ( $\pm 0.25$ )	15.98 ( $\pm 6.78$ )	0.68 ( $\pm 0.43$ )	3.05
	<i>C. finmarchicus</i> F (x3)	0	2.98 ( $\pm 0.17$ )	7.63 ( $\pm 3.51$ )	1.65 ( $\pm 0.33$ )	( $\pm 0.00$ )

### 3.7.2 Estimation of *Calanus* spp. community FP export

Following *Calanus* spp. abundances found at stations 19 (mid-bloom) and 31 (early-bloom), the contribution of FPC produced by the *Calanus* spp. community was highly variable (table 7). At the mid-bloom station 19, where *C. finmarchicus* females clearly dominated, their proportion of produced FPC that was exported to 40m was 4.31%, and therefore approximately 95% of their assumed FPC was not exported to 40m.

At the mid-bloom station 31, community production was analyzed for both *C. finmarchicus* females and *C. hyperboreus* females and CV (table 7). *C. finmarchicus* females were the most abundant in the upper water column, and their resulting community FPC



production exported was estimated to be 36.12% down to 40m. *C. hyperboreus*, on the other hand, were found in very low abundance in the upper 40m of the water column, whilst their FPC flux rate was relatively high (table 7). This resulted in a very large contribution to the FPC flux to 40m, 4403.57%.

Table 7. Integrated *Calanus* spp. community fecal pellet carbon (FPC) production (0-40m) in  $\text{mgC m}^{-2} \text{d}^{-1}$ , estimated for certain of the species investigated in the FP production experiment, at stations 19 and 31. Mean *Calanus* spp. abundances in depth interval 0-40m are given in  $\text{ind m}^{-2}$  (provided by B. Neihoff and S. Murawski (AWI)). Community production shown relative to *Calanus* spp. FPC exported to the 40m sediment trap, in  $\text{mgC m}^{-2} \text{d}^{-1}$ , and the estimated proportion of the community FPC exported to 40m depth, in %. \*High % community FPC export due to low abundances of *C. hyperboreus* in water column but with high FPC flux rate to the 40m sediment trap.

Station	<i>Calanus</i> sp. and life stage	Mean abundance 0-40m ( $\text{ind m}^{-2}$ )	Community FPC production 0-40m ( $\text{mgC m}^{-2} \text{d}^{-1}$ )	<i>Calanus</i> FPC export 40m ( $\text{mgC m}^{-2} \text{d}^{-1}$ )	% Community FPC exported to 40m
19	<i>C. finmarchicus</i> F	1588	20.10	0.87	4.31
31	<i>C. finmarchicus</i> F	1887	13.95	5.04	36.12
31	<i>C. hyperboreus</i> F+CV	66	0.98	43.29	4403.57*

## 4. Discussion

### 4.1 Successional characteristics of bloom events at the SSIZ

In the Arctic Ocean, biological productivity is largely determined by sea ice, making the seasonal sea ice zone (SSIZ) its most productive region (Wassmann and Reigstad 2011, Slagstad *et al.* 2015). Yet, precisely because of its seasonality, the productivity of the SSIZ is highly dynamic, varying over space and time.

The spring bloom has long been considered a rapidly propagating process at the SSIZ, depending on critical transmission of sunlight through the ice and water column stabilization of nutrient-rich surface waters as the ice recedes (Sverdrup 1953, Leu *et al.* 2015). With annual sea ice retreat becoming more extensive as a consequence of global warming, the greatest increases in primary productivity in the AO are found along the Eurasian perimeter (Wassmann and Reigstad 2011, Slagstad *et al.* 2015).

When classifying the development of spring blooms, certain characteristics are informative, including vertical nutrient profiles, size spectra of algal cells, vertical profile and proportion of phytodetritus (indicated by chlorophyll *a* and phaeopigments), and C:N ratios (Wassmann *et al.* 1999b, Hodal and Kristiansen 2008, Leu *et al.* 2015). In the current research, distinct assemblages of organic material were discovered over a relatively small area of the SSIZ. The stations located around the Yermak Plateau were in a pre-bloom phase, with high and homogenous concentrations of nutrients with depth, as well as low levels of chlorophyll *a* ( $<0.5 \text{ mg m}^{-3}$ ) that were approximately equivalent to phaeopigment concentrations. As the bloom progressed, surface nitrate declined while surface chlorophyll *a* levels increased. This progressed bloom scenario was found at stations further east, over the shelf break north of Svalbard. The proportion of phaeopigments became less significant, so that during mid-bloom conditions, the contribution of chlorophyll *a* was governing (appendix fig. A3). Additionally, the contribution of large cells generally increased as the bloom developed, which is in agreement with the tradition view of bloom succession (Sakshaug and Skjoldal 1989, Hodal and Kristiansen 2008, Leu *et al.* 2015).

However, the appearance of large algal cells and a dominance of chlorophyll *a* are inadequate in determining whether a bloom has developed (Wassmann *et al.* 1999b). Grouping of stations according to classical characteristics can be complex in the highly dynamic Arctic, where the conditions can vary greatly over space and time. Furthermore, station 47, in the deep Sofia basin, was statistically clustered and consequently grouped as early-bloom, but may have had a different bloom development than the other stations in the surrounding area. Suspended chlorophyll *a* and phaeopigments were found in intermediate concentrations ( $\sim 3 \text{ mgChla m}^{-3}$ ) in the upper water column, and quickly diminishing with

depth. However, the 10m nitrate concentration was found conspicuously low ( $1.64 \text{ mmolNO}_3 \text{ m}^{-3}$ ) but not depleted, which is not unusual for bloom conditions in the area, even when no strong stratification is present (Codispoti *et al.* 2013). The ice pack was concentrated (90-100%) and relatively thick (~1m) at this station, but notably the snow cover was very thin allowing for higher light transmittance (Peeken 2016). Additionally, this station was found to have the highest integrated chlorophyll *a* biomass in the sea ice and the under-ice waters (Peeken *pers. comm.*, Peeken 2016), which could explain the low surface nitrate concentrations. Consequently, it is likely that slow and steady melting of the ice (revealed by low surface salinities) had occurred in the Sofia basin, resulting in a slow and steady accumulation of ice algae and pelagic phytoplankton. This reveals that ice, and in particular snow cover, are major limiting factors of the early propagation of the spring bloom at the SSIZ, rather than nutrients. Therefore, and paradoxically, ice and snow transitions can be essential for both the rapid and intense propagation of the bloom, but also for its early termination or restriction. This is in line with a multi-year dataset compiled for Resolute Bay in the Canadian Arctic, where light, determined on a local scale by snow depth distribution, was significantly correlated to chlorophyll *a* accumulation in the ice and upper water column, during the early development phase of the bloom (Leu *et al.* 2015). However, as highlighted by Leu *et al.* (2015), a phytoplankton species composition at each station is necessary to further understand the state of bloom development at the stations, because the relative contributions ice algae and pelagic phytoplankton tend to vary as the bloom develops.

In light of this, another interesting observation was made at station 47. Upon retrieval of the sediment traps, large amounts of aggregated algae were found covering the line and additionally deployed equipment of the sediment traps (*personal observation*). This algal mass is suspected to be *Melosira arctica*, large chain-forming centric diatoms, which have been described to generate to very high biomass under the ice (both first-year and multi-year ice) (Nansen 1906; Melnikov and Bondarchuk 1987, Assmy *et al.* 2013, Leu *et al.* 2015). Further evidence to this was seen from the multiple CTD/RO casts made during this ice station, where large spikes in fluorescence were seen at depth (60-80m), but only present during some of the casts and at varying depths (appendix fig. A6). These fluorometric spikes can indicate sinking aggregates of *M. arctica*, occurring in patchy distribution. Furthermore, the benthic research done during this station revealed large amount of “fluff” on the surface sediment (N. Morata *pers. comm.*). This accumulation of fluff on the sea floor is often associated with fast-sinking aggregated algae and possibly *M. arctica*, whose importance in pelagic-benthic coupling from underneath ice is patchy but may be substantial, as observed over deep waters of the AO basin (Boetius *et al.* 2013). Therefore, to further understand how blooms and productivity propagate, as well as their fate in the Arctic ecosystem at the SSIZ,

the flux of organic material and the significance of heterotrophic consumers must be considered.

#### **4.2 Vertical export – Fate of the bloom**

As productivity is tightly coupled with seasonality, ice and snow cover at the SSIZ, the export of biogenic material can differ from the classical consensus for open water systems, as reviewed by Boyd and Trull (2007). The intensity and short duration of the spring blooms at the SSIZ tighten the connection between primary productivity and biogenic flux (Carroll and Carroll 2003). During the current study, a strong linear correlation between exported particulate organic carbon (POC) and chlorophyll *a* was found for all stations ( $R^2 > 0.98$ ,  $n=16$ ,  $y\text{-int.}=62.0$ ), indicating that the vertical flux of organic carbon follows the development of the bloom. Furthermore, the estimates of phytoplankton carbon (PPC) revealed increasing contribution of PPC as the bloom developed, ranging from 5-20% during pre-bloom to roughly 75% at mid-bloom conditions. This is in line with PPC contributions found by Reigstad *et al.* in the northern Barents Sea (2008) and in fjords in northern Norway (2000). Although microscopic analysis of phytoplankton species and cell volumes at each station would be required to support these estimates of PPC (e.g. following Strathmann 1967, and Smetacek 1975), they nevertheless suggest that as the bloom developed, PPC was the most important source to exported organic material.

In a study by Andreassen *et al.* (1996), sediment trap deployment in a transect northeast of Svalbard revealed that a significant contribution of POC flux was of terrestrial origin, where POC:PON ratios reached up to 26.6 (a:a). This exported material was assumed to originate from the Laptev Sea and advected just north of the current study region through the Transpolar Drift. The current study found no equivalent evidence of terrestrial material, as POC:PON ratios on average ranged from 7.7 to 8.8 from pre- to mid-bloom stations (table 5). Therefore, with a lack of terrestrial input, the current study highlights the importance of algal- and marine-originating material for the pelagic-benthic coupling in the current region of the SSIZ.

Pre-bloom conditions supported the lowest vertical export rates of POC (62-103 mgPOC  $\text{m}^{-3} \text{d}^{-1}$  at 30m), whilst the highest vertical export rates of POC were associated with the highest levels of phytodetritus at the mid-bloom stations (930-1165 mgPOC  $\text{m}^{-2} \text{d}^{-1}$  at 30m), dominated by large chlorophyll *a* cells. The mid-bloom stations, located on the Barents Sea shelf break north of Svalbard, demonstrated similar vertical export rates to those found in the MIZ of the central Barents Sea during spring and summer (Andreassen and Wassmann 1998, Olli *et al.* 2002), and higher than those of a similar area to the current

study (station XIV of Reigstad *et al.* 2008, and Hodal and Kristiansen 2008). The current study therefore demonstrates that the northern ice-covered Barents Sea shelf break can provide vertical export rates of organic material during the spring bloom that are comparable to the productive and shallower central Barents Sea.

Daily loss rates of both POC and chlorophyll *a* to 90m-depth generally increased as the bloom progressed, almost tripling from pre- to mid-bloom conditions. Daily loss rates ranged from roughly 0.5-3% and 0.5-5% for POC and chlorophyll *a* respectively, which is in line with loss rates discovered in the Arctic waters of the central Barents Sea by Olli *et al.* (2002). Additionally, the daily loss rates of the current study are comparable to those found in the northern Barents Sea by Reigstad *et al.* (2008) for an early-bloom stage, but higher in a mid-bloom stage. Nevertheless, daily loss rates <5% would suggest that, even under tight pelagic-benthic coupling at the SSIZ, important retention processes are taking place in the upper water column.

Stratification layers and nutriclines in the upper water column are often found to be hotspots of productivity due to the critical balance between light and nutrient availability (Sverdrup 1953). Consequently, retention processes, such as remineralization, grazing and degradation by heterotrophic consumers are often found closely associated with stratification layers (Wexels Riser *et al.* 2007, Reigstad *et al.* 2008). Summer melt periods at the SSIZ can create considerable pycno- and nutriclines associated with hotspots of productivity, can subsequently lead to higher retention rates than in open waters (Olli *et al.* 2002, Wassmann *et al.* 2003). In support of this, the current study demonstrates that as the bloom developed under the sea ice, the organic matter vertically exported in the shallower depths exceeded the flux to the deeper layers of the pelagic system, which is in line with previous studies of the MIZ (Olli *et al.* 2002). At the mid-bloom stations, significant decline in POC flux was found between the 40 and 60m sediment traps, indicating strong retention processes over the short vertical distances where accumulated organic biomass was the highest.

However, retention associated with stratification in the upper water column was not found at the early-bloom stations of this study. Station 31 had a prominent stratification layer between 25-40m, which did not seem to have significant influence over flux attenuation. On the contrary, the peak flux rates of chlorophyll *a* and phaeopigments were found at 60m. Furthermore, this station displayed an unproportionally high percentage loss rate in chlorophyll *a*, as a result of high flux to 90m despite having low integrated biomass. During the sampling of this ice station, the research vessel and ice flow drifted a great distance. Investigation into the multiple CTD/RO casts made during the station exposed that stratification was only evident in the water masses of the first cast, at the start of the station when samples for the suspended and thus integrated vertical profiles of chlorophyll *a* and

POC were collected. Later casts revealed no such stratification, but rather a notable increase in fluorescence (appendix fig. A7). Therefore, drifting of the sediment traps with the ice can have sampled multiple water masses, where the biogeochemistry and biomass of organic material varied. This highlights two concerns of the sampling methodology: (1) sampling of suspended biomass and calculations of integrated biomass represent a snapshot in time, and therefore, subsequent comparisons to exported material (integrating over 24 hours) and loss rates can be over- or underestimated. (2) Sediment traps that drift with the ice instead of the water column may not follow even a semi-Lagrangian drift, an assumption upon which the calculations of loss rates and fluxes are based (Olli *et al.* 2007, Wexels Riser *et al.* 2007).

Nevertheless, the sediment traps sampling over varying water columns will integrate spatial variability, and therefore be more representative of the processes taking place in the area. For example, the pre-bloom station 39, where low integrated chlorophyll *a* biomass was found, large cells contributed 140% of vertically exported chlorophyll *a* at 90m, suggesting patchy distribution of material. This proportion of large cells was not discovered from the suspended profile, highlighting that sediment traps can help to reveal spatial variability.

### **4.3 Impact of grazers**

The proportion of the spring bloom exported is largely determined by the retention capacity of the upper pelagic system, where activity of both producers and consumers is highest. Even though larger zooplankton can accelerate the flux by producing fast sinking FP (Turner *et al.* 2015), they can also attenuate the flux by mediating degradation processes by heterotrophic consumers (bacteria, dinoflagellates, ciliates, etc.) (Svensen *et al.* 2012). Filter-feeding zooplankton, like *Calanus* spp., may degrade FP through ingestion (coprophagy), mechanical break-up (coprorhexy) or by destroying the outer membrane of the FP (coprochaly) (Lampitt *et al.* 1990, Turner 2015). Previous studies have found that enhanced concentrations of copepods around the most chlorophyll *a*-rich depths may cause a higher degree of FP fragmentation, acting as a sort of retention filter in the most bioactive layers of the water column (Wexels Riser *et al.* 2007). Therefore, as the bloom develops and bioactive layers become more prominent, the retention filter was expected to strengthen respectively (fig.13).

At mid-bloom station 19, on the Barents Sea shelf break, *C. finmarchicus* was found dominant in the upper 40m and in comparable integrated abundances with previous studies in the Barents Sea (Olli *et al.* 2002, Wexels Riser *et al.* 2008). The FP production experiments at this station revealed that the community was producing FP, equivalent to roughly 20 mgFPC m<sup>-2</sup> d<sup>-1</sup>, yet only 4% of this FPC production was found sedimenting at

40m. This could be indicative of a strong retention filter above 40m, where the abundant copepods were mediating degradation of FP. Moreover, higher vertical FPC flux rate to 90m depth at this station was primarily produced by krill, accounting up to 6% of POC flux. Krill are often found significantly contributing to FPC flux below 90m (Wexles Riser *et al.* 2008). Even though krill have been observed to feed on ice algae as well as pelagic phytoplankton in the Bering Sea (Wang *et al.* 2015), their daily vertical migrations in the water column (Mauchline and Fisher 1969) may explain their FPC flux to 90m. Krill therefore may not contribute significantly to the retention filter.

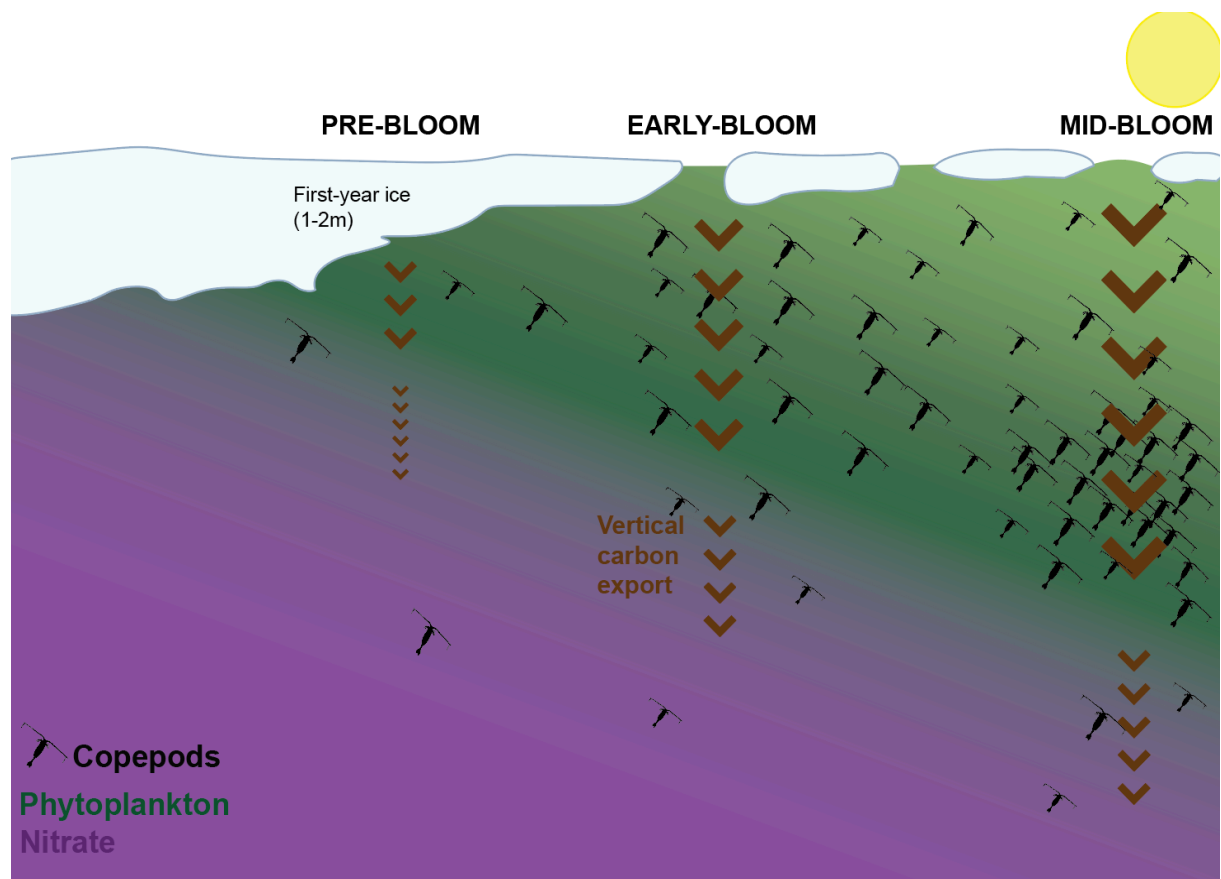


Figure 13. Visual interpretation of the anticipated bloom development and associated retention processes at the SSIZ. Grazers, here represented by calanoid copepods, strengthen retention processes as the bloom progresses in the most productively-active layer of the water column (where phytoplankton and grazers are abundant and nutrients remain available), resulting in a reduction of the bloom exported below this layer. Relative reduction of vertical carbon export in relation to bloom development is indicated by the relative size of the brown arrows.

The largest export of FPC flux was measured at the early-bloom stations, accounting for up to 25% of the flux of POC at 90m. At the early-bloom stations 27 and 31, little variation in FPC flux was seen between 40 and 90m. At both depths copepod FP dominated and therefore the steady flux suggests that little retention of FP occurred in the water between 40

and 90m. This may indicate that at earlier stages of bloom development, where chlorophyll *a* biomass was not as high, the strength of the retention filter is weaker (depicted by fig. 13). Moreover, at station 31, higher proportions of the FPC produced by the community of dominant *Calanus* spp. were found exported to 40m depth. For the community *C. finmarchicus*, which were abundant in the upper 40m, roughly 36% of the FPC produced were exported to 40m, suggesting less retention than at mid-bloom stations. The high 40m flux of FPC produced by *C. hyperboreus* is likewise indicative of lower retention processes. Unfortunately, the proportion of community FP exported cannot be compared, as the community-grazing estimates for *C. hyperboreus* could be under-quantified, leading to underestimated community production rates. The underestimation is suspected due to surprisingly low abundance numbers collected, which could be a result of sampling methods as the opening size of the multi-nets is suspected to be small enough for these large copepods to be able to escape (H. Flores *pers. comm.*). Additionally, station 31 was discovered to drift along variable concentrations of chlorophyll *a* (discussed in section 4.2). Therefore the live copepods and incubation water sampled for the FP production experiments, as well as the multi-net samples for community abundance, may not be truly representative for the producers and feeding environment of the FP material collected by the sediment traps throughout the station. This is in line with a discussion of the problems with sampling assumptions of semi-Langangian drifts by Olli *et al.* (2007).

Furthermore, at the early- and mid-bloom stations the flux of large FP became more prominent with depth, indicated by the increase in krill and large copepod pellets in the 90m sediment traps. This demonstrates how larger zooplankton can produce larger and thus more carbon-rich pellets, which are quickly exported. Previous studies have revealed that size of FP is the most significant in their capacity to be exported to depth (Stamieszkin *et al.* 2015). The current study therefore supports that the production of large fast-sinking FP, with high carbon content, can pass through the retention filter of the upper water column and thus provide a vital source of carbon to the benthos (Wexels Riser *et al.* 2008, Wiedmann *et al.* 2014, Turner 2015).

At the pre-bloom stations over the Yermak Plateau, FPC production and FPC flux were found very low, corresponding to the lack of food availability in the water (integrated chlorophyll *a* averaged 15-29 mg m<sup>-2</sup>, 0-90m). Moreover, these stations had a decrease in FPC export rates between 40 and 90m. All the pre-bloom stations appeared to have high abundances of large copepods, especially *C. hyperboreus* (*personal observation*, H. Flores *pers. comm.*). These grazers could therefore feed on any material present in the water (including other FP), retaining the material in the upper water column (fig. 13). This is in line with the importance of retention- and remineralization-mediated processes by grazers during



non- or pre-bloom conditions, previously discovered to be especially prominent in the ArW of the SSIZ (Wexels Riser *et al.* 2008).

The contribution of FPC flux to the total POC flux in the current study ranged from 0.5-24%, averaging ~7%, for all stations and depths. This average is higher than the average contributions previously found for the central AO, of <2% (Olli *et al.* 2007), within range of the northern Barents Sea and current study area, 10-27% (Wexels Riser *et al.* 2007, Wexels Riser *et al.* 2008), and lower of those described for the central Barents Sea, averaging roughly 40% (Wexels Riser *et al.* 2002). This suggests that the contribution of FPC to the total POC flux will be variable within time and space, but may generally diminish northward with the SSIZ. This trend may be the combined result of thickening ice and subsequent duration and intensity of the bloom (i.e. food availability), and advection patterns in the Arctic SSIZ domain steering zooplankton abundances as described by Wassmann *et al.* (2015).

Due to the highly variable development of the spring bloom and associated processes at the SSIZ, timing is sensitive. The capacity for development of intense blooms has been described to be an indication of mismatch, where production and consumption of the bloom is uneven (Wassmann 1998). Correspondingly, as the initiation and duration of spring bloom was found to vary significantly over space and time at the SSIZ, the timed response of grazers will fluctuate accordingly. At the assumed ice-bloom station 47 in the Sofia basin, a large increase in FPC flux was observed from 40 to 90m (from 1.1 to 36.5 mgFPC m<sup>-2</sup> d<sup>-1</sup> at 40 and 90m respectively). The contribution of FPC flux to the total POC flux also increased from 0.5 to 24% respectively, which was the highest change in FPC export with depth of all the stations. Considering the possible slow and steady propagation of both the ice-algae and pelagic bloom at this station (as discussed in section 4.1), this result suggests that grazers had time to respond to the development of the bloom and had been grazing significantly as production increased. It also demonstrates how grazing control could inhibit peak bloom development, as was discovered by Wassmann *et al.* (1999a) in a transect study across the north Norwegian shelf. Moreover, this result could be evidence to support that zooplankton (in this case copepods) will feed on patchy and carbon-rich ice algae aggregates, even those sinking in the water column, and indirectly contribute to their export out of the pelagic, as contemplated by Assmy *et al.* (2013). *C. hyperboreus*, which was dominant at station 47 (H. Flores *pers. comm.*), has been known not to vertically migrate under periods of midnight sun at the SSIZ (Blachowiak-Samolyk *et al.* 2006), but their possible placement in the water below 40m could have resulted in the low FPC flux to the 40m sediment trap. FPC analysis of the remaining sediment trap profile (to be completed after the submission of the current thesis) may give further insight into the vertical distribution of FPC producers in the water column.

#### 4.4 Outlook and future work

With the northward retreat of sea ice in the Arctic Ocean – a consequence of rapid climate warming – the largest changes in productivity are expected to take place in the northern portion of the present SSIZ (Wassmann and Reigstad 2011). The current study demonstrates that the bloom development and vertical carbon export at the northern Eurasian SSIZ is highly variable over space and time, and closely coupled with the dynamics of sea ice. The strength of the current study is the combined investigation of the suspended biomass, vertical export and potential retention processes involved during the most crucial period of bloom development at the SSIZ. Only through exploration of the components that both accelerate and attenuate the bloom and its fate at the SSIZ, can we form an understanding of the system and how it may transform under potential varying climatic conditions. Additionally, the current study took place in a region of SSIZ that is difficult to access during this time of year, and therefore previous knowledge of the onset of bloom development from this area is limited. Finally, the TRANSSIZ expedition was an international and highly interdisciplinary project, and the current study of suspended biomass and vertical export is an important contribution, particularly in linking sea ice, zooplankton and benthic studies.

In order to further assess the bloom and the subsequent vertical flux, additional analysis is needed. Firstly, detailed description of hydrological and physical conditions, such as ice, snow, drift, and water masses characteristics, at each station could reveal patterns of transmittance, sea ice melt, advection, and pycnoclines, which can control the structure of the blooms. As mentioned in section 4.1, species identification and community composition of ice algae and pelagic phytoplankton is required to further assess the relative contributions of primary producers during the development of the bloom.

Furthermore, it must be noted that the current study lacks data on the remaining community of zooplankton in the water column. *Calanus* species are commonly important in flux mediation (Wexels Riser *et al.* 2008), but without relative abundance to other zooplankton present, their community significance and subsequent flux mediation cannot be fully assessed. Nevertheless, the *Calanus* spp. abundance data for the remaining stations, which were not available for this study due to limited time for analysis, could give support to retention-filter assumptions at mid-bloom stations, and may reveal trends associated with earlier stages of bloom development.

Additionally, detailed depiction of zooplankton positioning in the water column, in distinct depth intervals, would give insight into the effect of diel vertical migration of grazers and their subsequent FP production and flux. The remaining sediment traps samples (from 30, 60 and 200m depths) should be analyzed to get a better understanding of the flux of FP

and its contribution to the total POC flux throughout the vertical profile studied. The proportion of broken or degraded FP in the sediment traps should also be examined to support degradation by zooplankton-mediated processes.

Lastly, this study also reveals how variable the conditions of the SSIZ can be. This study uncovers only a snapshot within space and time, and consequently, inter-annual and spatial variations could reveal alternative scenarios. Further investigations into the northern regions of the Eurasian SSIZ, both deeper into the basin of the AO and over a longer time period of the summer, would give a more comprehensive insight into entire development of the spring bloom, as well as into the consequences of future sea ice retreat.

## 5. Conclusion

The current wide-ranging investigation in the northern region of the Eurasian SSIZ, which is difficult to access during early spring, revealed that late-May and June are important months for the onset and development of the spring bloom and flux of organic matter under the ice. The biogenic biomass and vertical flux were found to be more sensitive to changes in ice and, in particular, snow cover, than nitrate concentrations. Small variation in ice and snow cover not only influenced the magnitude of bloom conditions, but seemingly also the timing and progression at which blooms occur.

Distinct assemblages of organic material were discovered over a relatively small area of the northern SSIZ. Vertical carbon export rates were found to vary significantly over varying bloom stages, both in terms of magnitude and composition, but were generally comparable vertical export rates of the productive and shallower central Barents Sea. The potential for vertical export to depth was greatest, in terms of daily loss and flux rates, at the stations on the Barents Sea shelf break found to be in mid-bloom development, and lowest at those in pre-bloom condition over the Yermak Plateau. Generally, PPC was found to be a more important component to the vertical POC flux than FPC, especially as the bloom developed.

As the bloom progressed from a pre- to mid-bloom condition, the organic matter vertically exported in the shallower depths exceeded the flux to the deeper layers of the pelagic system, indicating retention in the upper water column. The proportion of *Calanus finmarchicus* community-produced FPC that was exported to 40m, decreased from 36% to 4% from early- to mid-bloom conditions, suggesting stronger zooplankton-mediated retention as the bloom intensifies. Additionally, under slower bloom development, grazers appeared to be effectively controlling and inhibiting the accumulation of biogenic biomass and subsequent vertical flux.

Overall, the current study describes production, vertical export and retention processes occurring in a previously unstudied section of the SSIZ during onset of the spring bloom. Additional studies into sea ice algae, pelagic phytoplankton and zooplankton community composition at the stations would give greater insight into the important actors and interactions in the vertical export of material, in the upper waters of the SSIZ.

## References

- Aagaard, K., Foldvik, A. and Hillman, S.R., 1987. The West Spitsbergen Current: disposition and water mass transformation. *Journal of Geophysical Research: Oceans*, 92(C4), pp.3778-3784.
- Andreassen, I., Nöthig, E.M. and Wassmann, P., 1996. Vertical particle flux on the shelf off northern Spitsbergen, Norway. *Marine ecology-progress series*, 137, pp.215-228.
- Andreassen, I.J. and Wassmann, P., 1998. Vertical flux of phytoplankton and particulate biogenic matter in the marginal ice zone of the Barents Sea in May 1993. *Marine Ecology Progress Series*, 170, pp.1-14.
- Arashkevich, E., Wassmann, P., Pasternak, A. and Wexels Riser, C., 2002. Seasonal and spatial changes in biomass, structure, and development progress of the zooplankton community in the Barents Sea. *Journal of Marine Systems*, 38(1), pp.125-145.
- Arrigo, K.R., Perovich, D.K., Pickart, R.S., Brown, Z.W., van Dijken, G.L., Lowry, K.E., Mills, M.M., Palmer, M.A., Balch, W.M., Bahr, F. and Bates, N.R., 2012. Massive phytoplankton blooms under Arctic sea ice. *Science*, 336(6087), pp.1408-1408.
- Assmy, P., Smetacek, V., Montresor, M., Klaas, C., Henjes, J., Strass, V.H., Arrieta, J.M., Bathmann, U., Berg, G.M., Breitbarth, E. and Cisewski, B., 2013. Thick-shelled, grazer-protected diatoms decouple ocean carbon and silicon cycles in the iron-limited Antarctic Circumpolar Current. *Proceedings of the National Academy of Sciences*, 110(51), pp.20633-20638.
- Barber, D.G., Hop, H., Mundy, C.J., Else, B., Dmitrenko, I.A., Tremblay, J.E., Ehn, J.K., Assmy, P., Daase, M., Candlish, L.M. and Rysgaard, S., 2015. Selected physical, biological and biogeochemical implications of a rapidly changing Arctic Marginal Ice Zone. *Progress in Oceanography*, 139, pp.122-150.
- Berge, J., Renaud, P.E., Darnis, G., Cottier, F., Last, K., Gabrielsen, T.M., Johnsen, G., Seuthe, L., Weslawski, J.M., Leu, E. and Moline, M., 2015. In the dark: A review of ecosystem processes during the Arctic polar night. *Progress in Oceanography*, 139, pp.258-271.
- Beszczynska-Möller, A., Fahrbach, E., Schauer, U. and Hansen, E., 2012. Variability in Atlantic water temperature and transport at the entrance to the Arctic Ocean, 1997–2010. *ICES Journal of Marine Science: Journal du Conseil*, p.fss056.

- Blachowiak-Samolyk, K., Kwasniewski, S., Richardson, K., Dmoch, K., Hansen, E., Hop, H., Falk-Petersen, S. and Mouritsen, L.T., 2006. Arctic zooplankton do not perform diel vertical migration (DVM) during periods of midnight sun. *Marine Ecology Progress Series*, 308, pp.101-116.
- Bluhm, B.A., Kosobokova, K.N. and Carmack, E.C., 2015. A tale of two basins: An integrated physical and biological perspective of the deep Arctic Ocean. *Progress in Oceanography*, 139, pp.89-121.
- Boetius, A., Albrecht, S., Bakker, K., Bienhold, C., Felden, J., Fernández-Méndez, M., Hendricks, S., Katlein, C., Lalande, C., Krumpen, T. and Nicolaus, M., 2013. Export of algal biomass from the melting Arctic sea ice. *Science*, 339(6126), pp.1430-1432.
- Boyd, P.W. and Trull, T.W., 2007. Understanding the export of biogenic particles in oceanic waters: Is there consensus? *Progress in Oceanography*, 72(4), pp.276-312.
- Carroll, M.L. and Carroll, J., 2003. The Arctic Seas. *Biogeochemistry of marine systems*. Blackwell Publishing, Oxford, pp.126-156.
- Codispoti, L.A., Kelly, V., Thessen, A., Matrai, P., Suttles, S., Hill, V., Steele, M. and Light, B., 2013. Synthesis of primary production in the Arctic Ocean: III. Nitrate and phosphate based estimates of net community production. *Progress in Oceanography*, 110, pp.126-150.
- Coppola, L., Roy-Barman, M., Wassmann, P., Mulsow, S. and Jeandel, C., 2002. Calibration of sediment traps and particulate organic carbon export using <sup>234</sup>Th in the Barents Sea. *Marine Chemistry*, 80(1), pp.11-26.
- De La Rocha, C.L. and Passow, U., 2007. Factors influencing the sinking of POC and the efficiency of the biological carbon pump. *Deep Sea Research Part II: Topical Studies in Oceanography*, 54(5), pp.639-658.
- Edler, L., 1979. Recommendations on methods for marine biological studies in the Baltic Sea. Phytoplankton and chlorophyll. *Publication-Baltic Marine Biologists BMB (Sweden)*.
- Fer, I., Skogseth, R. and Geyer, F., 2010. Internal waves and mixing in the marginal ice zone near the Yermak Plateau\*. *Journal of Physical Oceanography*, 40(7), pp.1613-1630.
- Greenacre, M. and Primicerio, R., 2013. *Multivariate analysis of ecological data*. Fundación BBVA.

- Hodal, H. and Kristiansen, S., 2008. The importance of small-celled phytoplankton in spring blooms at the marginal ice zone in the northern Barents Sea. *Deep Sea Research Part II: Topical Studies in Oceanography*, 55(20), pp.2176-2185.
- Holm-Hansen, O. and Riemann, B., 1978. Chlorophyll a determination: improvements in methodology. *Oikos*, pp.438-447.
- Kwasniewski, S., Hop, H., Falk-Petersen, S. and Pedersen, G., 2003. Distribution of Calanus species in Kongsfjorden, a glacial fjord in Svalbard. *Journal of Plankton Research*, 25(1), pp.1-20.
- Lalande, C., 2006. *Vertical export of biogenic in the Barents and Chukchi Seas* (Doctoral dissertation, PhD. Thesis, University of Knoxville, Tennessee, USA).
- Lampitt, R.S., Noji, T. and Von Bodungen, B., 1990. What happens to zooplankton faecal pellets? Implications for material flux. *Marine Biology*, 104(1), pp.15-23.
- Leu, E., Mundy, C.J., Assmy, P., Campbell, K., Gabrielsen, T.M., Gosselin, M., Juul-Pedersen, T. and Gradinger, R., 2015. Arctic spring awakening—Steering principles behind the phenology of vernal ice algal blooms. *Progress in Oceanography*, 139, pp.151-170.
- Mauchline, J., and Fisher, L.R. 1969. The biology of euphausiids. *Adv. Mar. Biol.*, 7, pp.1–454.
- Melnikov, I.A. and Bondarchuk, L.L., 1987. Ecology of mass accumulations of colonial diatom algae under drifting Arctic ice. *Oceanology*, 27, pp.233-236.
- Miquel, J.C., Gasser, B., Martín, J., Marec, C., Babin, M., Fortier, L. and Forest, A., 2015. Downward particle flux and carbon export in the Beaufort Sea, Arctic Ocean; the role of zooplankton. *Biogeosciences*, 12(16), pp.5103-5117.
- Müller, J., Massé, G., Stein, R. and Belt, S.T., 2009. Variability of sea-ice conditions in the Fram Strait over the past 30,000 years. *Nature Geoscience*, 2(11), pp.772-776.
- NSIDC, 2015. "Arctic Sea Ice Reaches Fourth Lowest Minimum | Arctic Sea Ice News And Analysis". *Nsidc.org*. N.p., 2015. Web. 10 May 2016.
- Nansen, F., 1906. *Northern waters: Captain Roald Amundsen's oceanographic observations in the Arctic Seas in 1901. With a discussion of the origin of the Bottom-Waters of the Northern Seas* (No. 3). In commission by Jacob Dybwad.
- Noji, T.T., Rey, F., Miller, L.A., Børsheim, K.Y. and Urban-Rich, J., 1999. Fate of biogenic carbon in the upper 200m of the central Greenland Sea. *Deep Sea Research Part II: Topical Studies in Oceanography*, 46(6), pp.1497-1509.

- Olli, K., Wexels Riser, C., Wassmann, P., Ratkova, T., Arashkevich, E. and Pasternak, A., 2002. Seasonal variation in vertical flux of biogenic matter in the marginal ice zone and the central Barents Sea. *Journal of Marine Systems*, 38(1), pp.189-204.
- Olli, K., Wassmann, P., Reigstad, M., Ratkova, T.N., Arashkevich, E., Pasternak, A., Matrai, P.A., Knulst, J., Tranvik, L., Klais, R. and Jacobsen, A., 2007. The fate of production in the central Arctic Ocean—top—down regulation by zooplankton expatriates?. *Progress in Oceanography*, 72(1), pp.84-113.
- Peeken, I., 2016. The Expedition PS92 of the Research Vessel POLARSTERN to the Arctic Ocean in 2015. *Berichte zur Polar-und Meeresforschung= Reports on polar and marine research*, 694.
- Rand, M.C., Greenberg, A.E. and Taras, M.J., 1975. Standard methods for the examination of water and waste water. *Franson, M., American Public Health Association, American Water Works Association, Water Pollution Control Federation, Washington*, pp.1193.
- Reigstad, M., Wexles Riser, C., Wassmann, P. and Ratkova, T., 2008. Vertical export of particulate organic carbon: attenuation, composition and loss rates in the northern Barents Sea. *Deep Sea Research Part II: Topical Studies in Oceanography*, 55(20), pp.2308-2319.
- Renaud, P.E., Morata, N., Carroll, M.L., Denisenko, S.G. and Reigstad, M., 2008. Pelagic—benthic coupling in the western Barents Sea: processes and time scales. *Deep Sea Research Part II: Topical Studies in Oceanography*, 55(20), pp.2372-2380.
- Rudels, B., 2012. Arctic Ocean circulation and variability—advection and external forcing encounter constraints and local processes. *Ocean Science*, 8(2), p.261.
- Sakshaug, E. and Skjoldal, H.R., 1989. Life at the ice edge. *Ambio (Sweden)*.
- Sakshaug, E., 2004. Primary and secondary production in the Arctic Seas. In *The organic carbon cycle in the Arctic Ocean* (pp. 57-81). Springer Berlin Heidelberg.
- Sakshaug, E., Johnsen, G.H. and Kovaks, K.M., 2009. *Ecosystem Barents Sea*. Tapir Academic, p.201
- Slagstad, D., Wassmann, P.F. and Ellingsen, I., 2015. Physical constrains and productivity in the future Arctic Ocean. *Frontiers in Marine Science*, 2, p.85.
- Smetacek, V. 1975. Die Sukzession des Phytoplanktons in der westlichen Kieler Bucht. *Ph.D. thesis, University of Kiel*.
- Smetacek, V. and Hendrikson, P., 1979. Composition of particulate organic-matter in kiel bight in relation to phytoplankton succession. *Oceanologica acta*, 2(3), pp.287-298.



- Soltwedel, T., Mokievsky, V. and Schewe, I., 2000. Benthic activity and biomass on the Yermak Plateau and in adjacent deep-sea regions northwest of Svålbard. *Deep Sea Research Part I: Oceanographic Research Papers*, 47(9), pp.1761-1785.
- Stamieszkin, K., Pershing, A.J., Record, N.R., PilskaIn, C.H., Dam, H.G. and Feinberg, L.R., 2015. Size as the master trait in modeled copepod fecal pellet carbon flux. *Limnology and Oceanography*, 60(6), pp.2090-2107.
- Strathmann, R.R., 1967. Estimating the organic carbon content of phytoplankton from cell volume or plasma volume. *Limnol. Oceanogr.* 12, pp. 411–418.
- de Steur, L., Hansen, E., Mauritzen, C., Beszczynska-Möller, A. and Fahrbach, E., 2014. Impact of recirculation on the East Greenland Current in Fram Strait: Results from moored current meter measurements between 1997 and 2009. *Deep Sea Research Part I: Oceanographic Research Papers*, 92, pp.26-40.
- Svensen, C., Riser, C.W., Reigstad, M. and Seuthe, L., 2012. Degradation of copepod faecal pellets in the upper layer: Role of microbial community and *Calanus finmarchicus*. *Marine Ecology Progress Series*, 462, pp.39-49.
- Sverdrup, H.U., 1953. On conditions for the vernal blooming of phytoplankton. *Journal du Conseil*, 18(3), pp.287-295.
- Tamelander, T., Reigstad, M., Hop, H. and Ratkova, T., 2009. Ice algal assemblages and vertical export of organic matter from sea ice in the Barents Sea and Nansen Basin (Arctic Ocean). *Polar biology*, 32(9), pp.1261-1273.
- Turner, J.T., 2015. Zooplankton fecal pellets, marine snow, phytodetritus and the ocean's biological pump. *Progress in Oceanography*, 130, pp.205-248.
- Walczowski, W., 2013. Frontal structures in the West Spitsbergen Current margins. *Ocean Science*, 9(6), pp.957-975.
- Wang, S.W., Budge, S.M., Iken, K., Gradinger, R.R., Springer, A.M. and Wooller, M.J., 2015. Importance of sympagic production to Bering Sea zooplankton as revealed from fatty acid-carbon stable isotope analyses. *Marine Ecology Progress Series*, 518, pp.31-50.
- Wassmann, P., 1998. Retention versus export food chains: processes controlling sinking loss from marine pelagic systems. In *Eutrophication in Planktonic Ecosystems: Food Web Dynamics and Elemental Cycling* (pp. 29-57). Springer Netherlands.
- Wassmann, P., Andreassen, I.J., Rey, F. and Høisæter, T., 1999a. Seasonal variation of nutrients and suspended biomass on a transect across Nordvestbasken, north Norwegian shelf, in 1994. *Sarsia*, 84(3-4), pp.199-212.

- Wassmann, P., Ratkova, T., Andreassen, I., Vernet, M., Pedersen, G. and Rey, F., 1999b. Spring bloom development in the marginal ice zone and the central Barents Sea. *Marine Ecology*, 20(3-4), pp.321-346.
- Wassmann, P., Olli, K., Wexels Riser, C. and Svensen, C., 2003. Ecosystem function, biodiversity and vertical flux regulation in the twilight zone. In *Marine Science Frontiers for Europe* (pp. 279-287). Springer Berlin Heidelberg.
- Wassmann, P., Slagstad, D., Wexels Riser, C. and Reigstad, M., 2006. Modelling the ecosystem dynamics of the Barents Sea including the marginal ice zone: II. Carbon flux and interannual variability. *Journal of Marine Systems*, 59(1), pp.1-24.
- Wassmann, P., Slagstad, D. and Ellingsen, I., 2010. Primary production and climatic variability in the European sector of the Arctic Ocean prior to 2007: preliminary results. *Polar Biology*, 33(12), pp.1641-1650.
- Wassmann, P. and Reigstad, M., 2011. Future Arctic Ocean seasonal ice zones and implications for pelagic-benthic coupling. *Oceanography*, 24, pp. 220–231.
- Wassmann, P., Kosobokova, K.N., Slagstad, D., Drinkwater, K.F., Hopcroft, R.R., Moore, S.E., Ellingsen, I., Nelson, R.J., Carmack, E., Popova, E. and Berge, J., 2015. The contiguous domains of Arctic Ocean advection: trails of life and death. *Progress in Oceanography*, 139, pp.42-65.
- Wexels Riser, C., Wassmann, P., Olli, K., Pasternak, A. and Arashkevich, E., 2002. Seasonal variation in production, retention and export of zooplankton faecal pellets in the marginal ice zone and central Barents Sea. *Journal of marine Systems*, 38(1), pp.175-188.
- Wexels Riser, C., Reigstad, M., Wassmann, P., Arashkevich, E. and Falk-Petersen, S., 2007. Export or retention? Copepod abundance, faecal pellet production and vertical flux in the marginal ice zone through snap shots from the northern Barents Sea. *Polar Biology*, 30(6), pp.719-730.
- Wexels Riser, C., Wassmann, P., Reigstad, M. and Seuthe, L., 2008. Vertical flux regulation by zooplankton in the northern Barents Sea during Arctic spring. *Deep Sea Research Part II: Topical Studies in Oceanography*, 55(20), pp.2320-2329.
- Wexels Riser, C., Reigstad, M. and Wassmann, P., 2010. Zooplankton-mediated carbon export: A seasonal study in a northern Norwegian fjord. *Marine Biology Research*, 6(5), pp.461-471.

Wiedmann, I., Reigstad, M., Sundfjord, A. and Basedow, S., 2014. Potential drivers of sinking particle's size spectra and vertical flux of particulate organic carbon (POC): Turbulence, phytoplankton, and zooplankton. *Journal of Geophysical Research: Oceans*, 119(10), pp.6900-6917.

Wilson, S.E., Steinberg, D.K. and Buesseler, K.O., 2008. Changes in fecal pellet characteristics with depth as indicators of zooplankton repackaging of particles in the mesopelagic zone of the subtropical and subarctic North Pacific Ocean. *Deep Sea Research Part II: Topical Studies in Oceanography*, 55(14), pp.1636-1647.

## Appendix

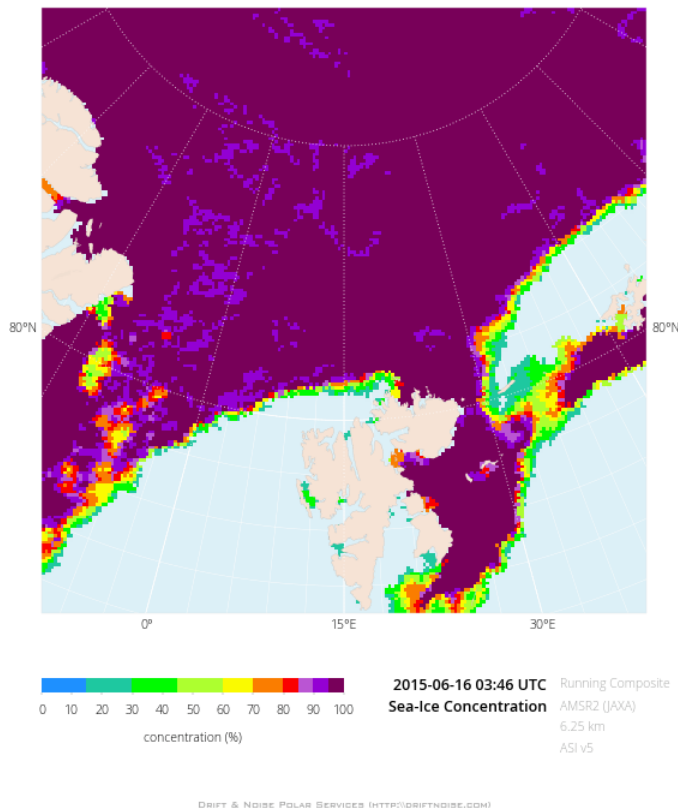


Figure A1. Sea ice concentration of Eurasian Arctic SSIZ, including the research area, for 16.06.2015. Sea ice concentration, in %, is shown. Image provided by Drift & Noise Polar Services GmbH.

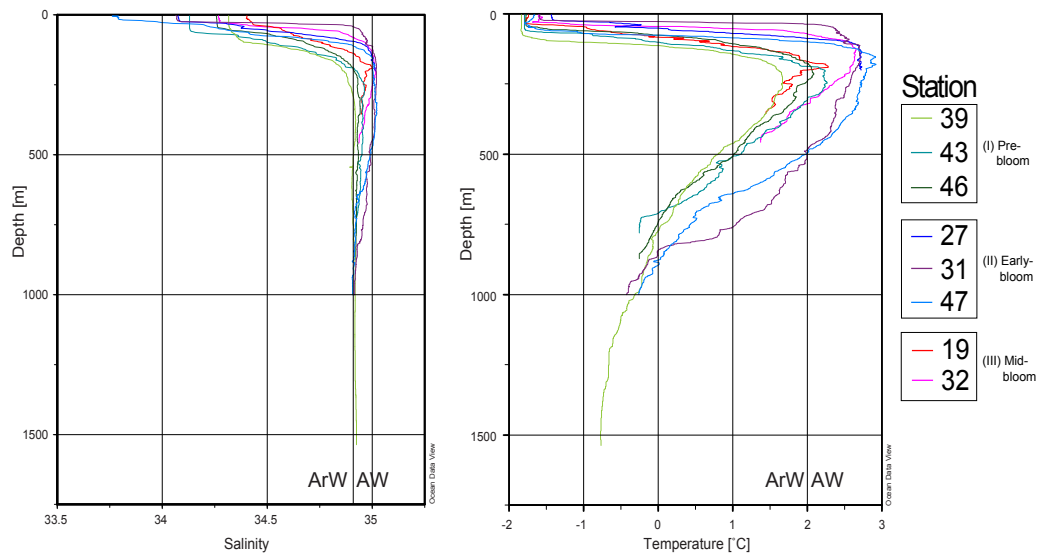


Figure A2. Full salinity (S) and temperature (T, in °C) profiles for each sea ice station. The profiles represent the CTD/RO casts from which samples were collected for analysis of suspended biomass. Vertical lines drawn at  $S=34.92$  and  $T=2^{\circ}\text{C}$  to mark boundary for the classifications of Arctic water (ArW) and Atlantic water (AW) (when both requirements of S and T are fulfilled). Stations color-coded according to bloom developmental stage (index).

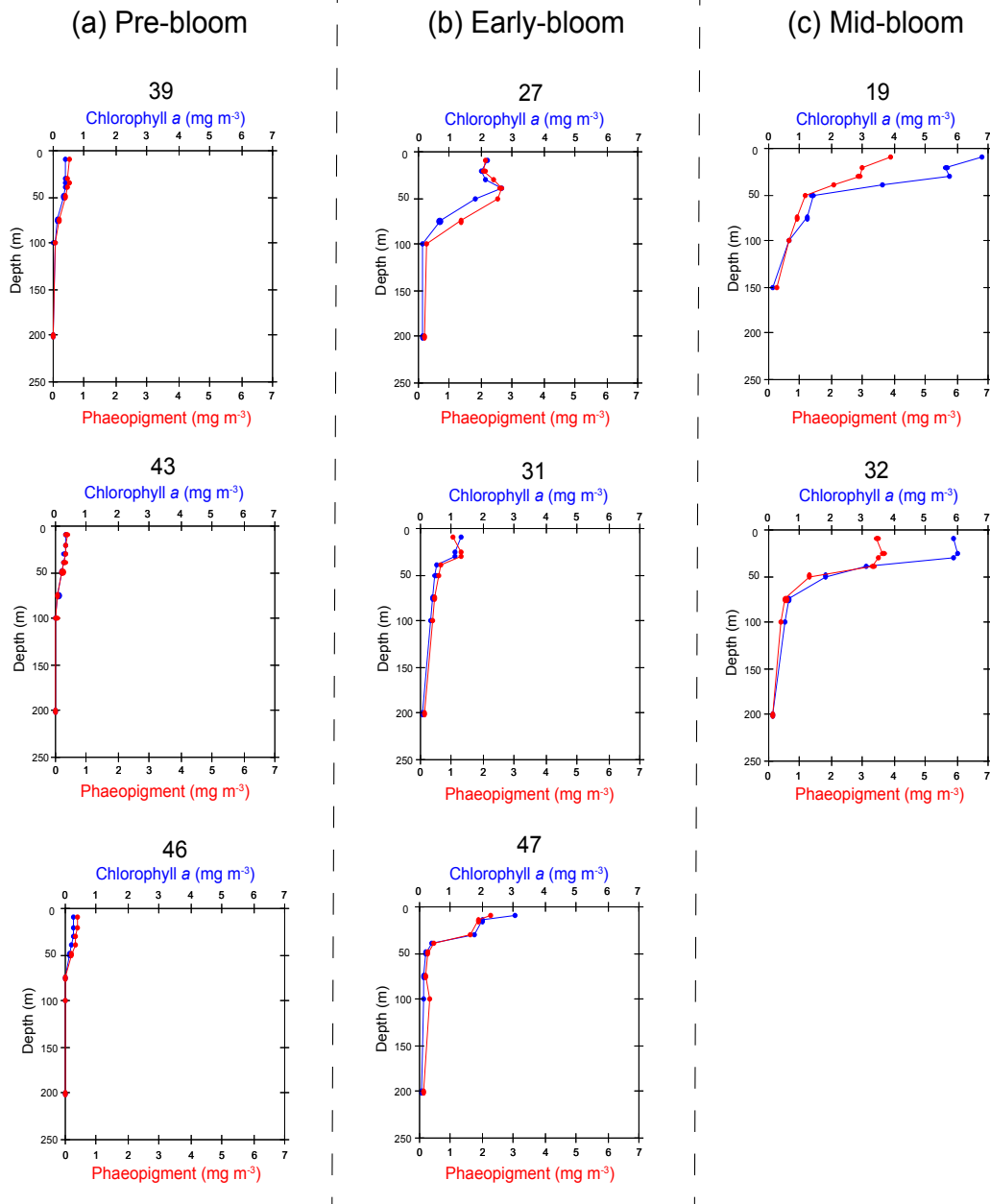


Figure A3. Vertical profiles of average suspended chlorophyll *a* (blue upper axis) and phaeopigments (red lower axis), in  $\text{mg m}^{-3}$ , for each sea ice station. Stations grouped according to bloom development phase: (a) pre-bloom stations, (b) early-bloom stations, and (c) mid-bloom stations.

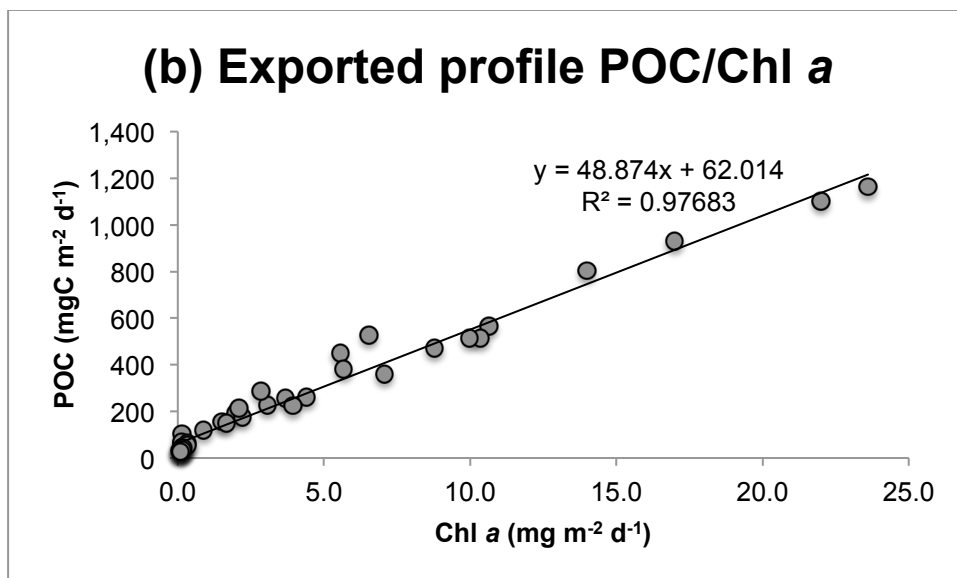
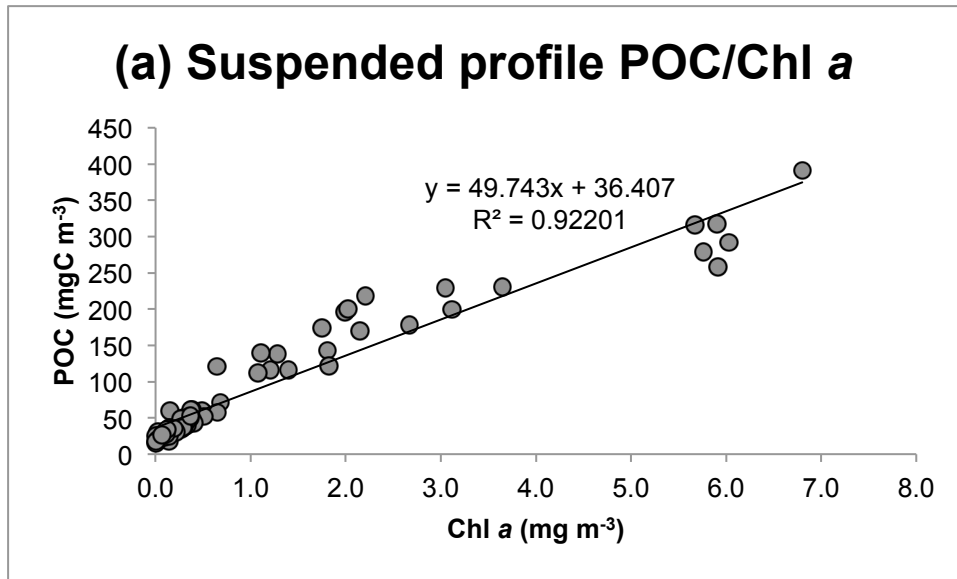


Figure A4. Relationship between particulate organic carbon and chlorophyll a (POC/Chl a), given by regression of all sea ice stations and depths, for (a) the suspended and (b) exported material.

Table A8. Overview of export rates of chlorophyll *a* (Chl *a*), particulate organic carbon (POC), fecal pellet carbon (FPC) and estimated phytoplankton carbon (PPC), in mg m<sup>-2</sup> d<sup>-1</sup>, as well as contribution of large fraction of Chl *a* (>10µm) in %, POC:PON ratios, and proportion of PPC to the POC export in %, for all sea ice station and depths sampled. Export rates and ratios are given as averages with standard deviation (SD, *n*=3). \*Note high proportion in Chl *a* >10µm 90m-sample at station 39, indicating possible patchiness in exported profile.

Station (Group)	Depth (m)	Chl <i>a</i> ± SD (mg m <sup>-2</sup> d <sup>-1</sup> )	% Chl <i>a</i> >10µm	POC ± SD (mgC m <sup>-2</sup> d <sup>-1</sup> )	POC:PON ± SD (a:a)	FPC (mgC m <sup>-2</sup> d <sup>-1</sup> )	Est. PPC (mgC m <sup>-2</sup> d <sup>-1</sup> )	% PPC/POC
19 (III)	30	16.99 ± 0.47	74	930.1 ± 28.5	7.58 ± 0.02		628.9	68
	40	13.99 ± 1.21	85	804.2 ± 25.1	7.57 ± 0.07	3.05	518.0	64
	60	10.63 ± 0.81	70	566.6 ± 6.5	7.34 ± 0.15		393.6	69
	90	8.77 ± 0.94	86	472.1 ± 18.6	7.31 ± 0.16	29.30	324.7	69
27 (II)	30	5.56 ± 0.05	43	450.3 ± 4.8	7.08 ± 0.15		205.7	46
	40	6.55 ± 0.04	36	526.3 ± 40.8	6.95 ± 0.20	26.09	242.5	46
	60	5.66 ± 0.15	49	382.5 ± 2.9	7.11 ± 0.22		209.6	55
	90	4.40 ± 0.17	60	261.8 ± 74.8	7.80 ± 0.48	24.48	162.7	62
	200	2.00 ± 0.03	65	192.4 ± 8.9	7.75 ± 0.16		74.0	38
31 (II)	30	3.06 ± 0.09	45	226.7 ± 3.7	6.71 ± 0.14		113.1	50
	40	3.68 ± 0.09	56	256.9 ± 10.9	7.38 ± 0.23	38.55	136.2	53
	60	2.20 ± 0.06	66	175.8 ± 21.2	7.03 ± 0.12		81.6	46
	90	3.95 ± 0.29	54	225.5 ± 17.3	7.19 ± 0.11	43.39	146.0	65
	200	1.52 ± 0.12	81	156.8 ± 17.7	7.57 ± 0.36		56.1	36
32 (III)	30	23.61 ± 0.60	42	1164.6 ± 94.9	7.86 ± 0.32		873.9	75
	40	22.00 ± 0.27	41	1099.6 ± 20.6	8.02 ± 0.16	3.22	814.4	74
	60	10.36 ± 0.75	52	512.6 ± 31.1	8.07 ± 0.28		383.6	75
	90	9.99 ± 0.19	61	512.7 ± 29.4	8.03 ± 0.17	12.83	369.6	72
	200	7.06 ± 0.11	35	359.0 ± 29.3	8.02 ± 0.14		261.4	73
39 (I)	30	0.15 ± 0.02	30	102.9 ± 62.1	9.09 ± 1.80		5.5	5
	40	0.14 ± 0.00	48	62.2 ± 20.6	9.36 ± 3.38	6.43	5.3	8
	60	0.13 ± 0.02	15	30.7 ± 3.2	7.51 ± 0.89		4.8	16
	90	0.12 ± 0.01	140*	31.2 ± 1.5	8.96 ± 1.11	0.64	4.6	15
	200	0.09 ± 0.01	4	31.8 ± 12.4	10.06 ± 2.96		3.2	10
43 (I)	30	0.13 ± 0.01	25	67.4 ± 6.4	11.32 ± 3.15		4.8	7
	40	0.17 ± 0.02	15	49.6 ± 4.2	8.07 ± 0.43	0.15	62	12
	60	0.14 ± 0.01	15	44.2 ± 3.5	8.36 ± 0.24		5.3	12
	90	0.07 ± 0.01	9	31.3 ± 1.1	11.04 ± 0.68	0.00	2.6	8
	200	0.08 ± 0.01	6	30.5 ± 4.4	9.22 ± 0.97		3.1	10
46 (I)	30	0.33 ± 0.02	17	62.4 ± 1.2	8.03 ± 0.45		12.2	20
	40	0.33 ± 0.02	16	55.1 ± 13.9	7.83 ± 1.89	5.99	12.0	22
	60	0.20 ± 0.03	15	42.6 ± 4.0	7.20 ± 0.59		7.6	18
	90	0.14 ± 0.01	18	35.3 ± 2.9	8.12 ± 0.13	0.00	5.3	15
	200	0.18 ± 0.00	16	26.7 ± 2.0	8.11 ± 0.69		3.0	11
47 (II)	30	2.85 ± 0.10	28	287.2 ± 14.8	7.77 ± 0.31		105.7	37
	40	2.09 ± 0.05	42	213.7 ± 2.9	7.61 ± 0.04	4.27	77.4	36
	60	1.56 ± 0.10	43				57.6	
	90	1.67 ± 0.09	58	149.5 ± 43.3	8.37 ± 0.98	53.35	61.8	41
	200	0.88 ± 0.03	62	120.4 ± 1.0	8.11 ± 0.58		32.5	27

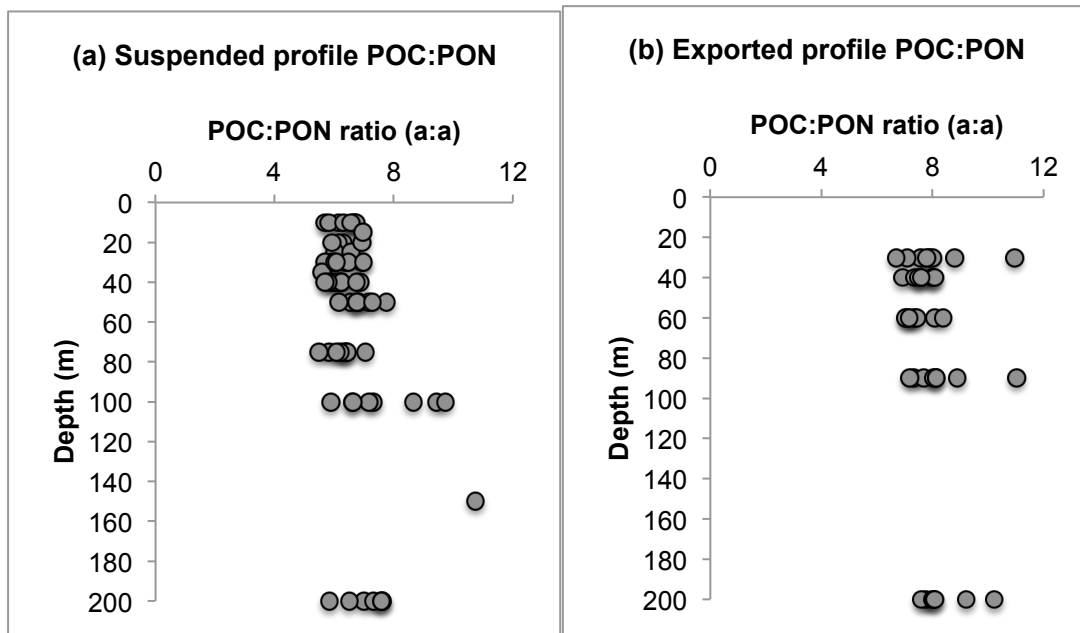


Figure A5. Particulate organic carbon to nitrogen (POC:PON) ratios, including all sea ice stations and depths sampled, for (a) suspended and (b) exported profiles

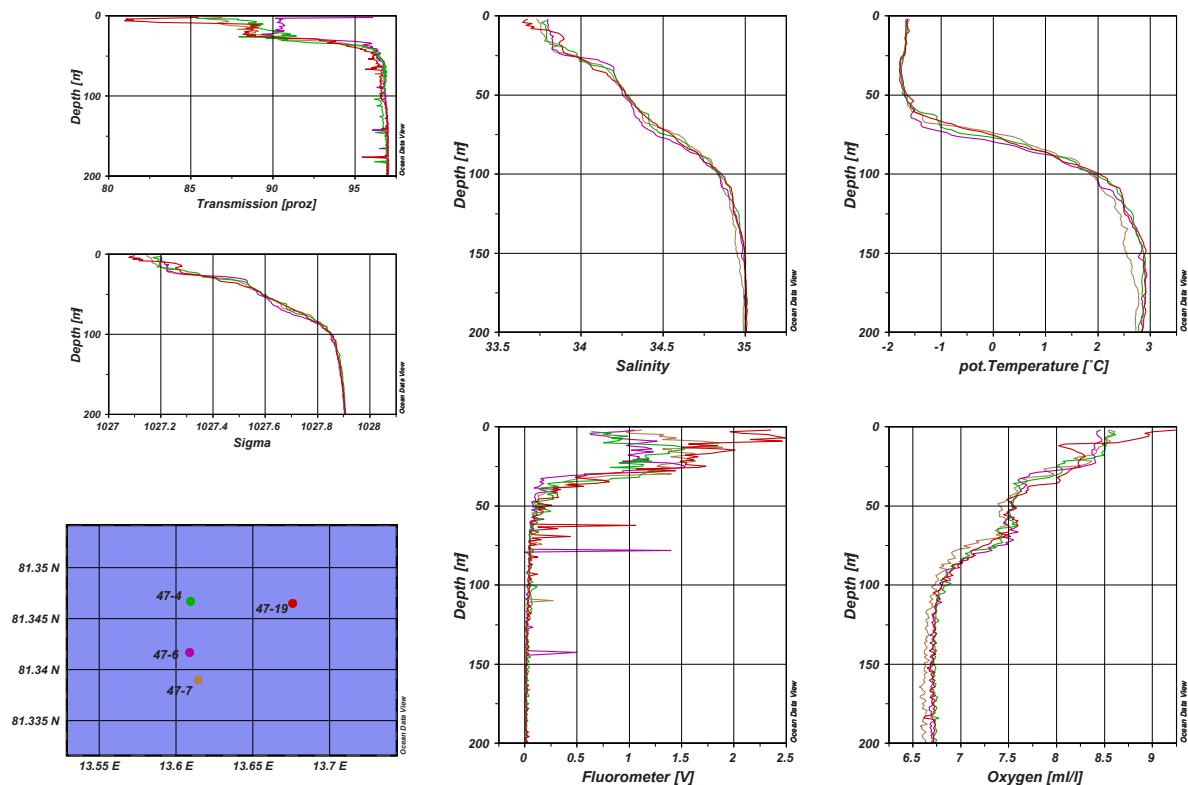


Figure A6. Overview of the four CTD/RO casts made at station 47, in the Sofia Basin (map, lower left corner). Profiles shown for the upper 200m of the water column: transmission (in proz), sigma (sea water density), salinity, potential temperature (in °C), fluorescence (in V) and oxygen concentration (in  $\text{ml l}^{-1}$ ). Cast 47-4 was sampled for suspended biomass profile. Note spikes in fluorescence at casts 47-6 and 47-19.



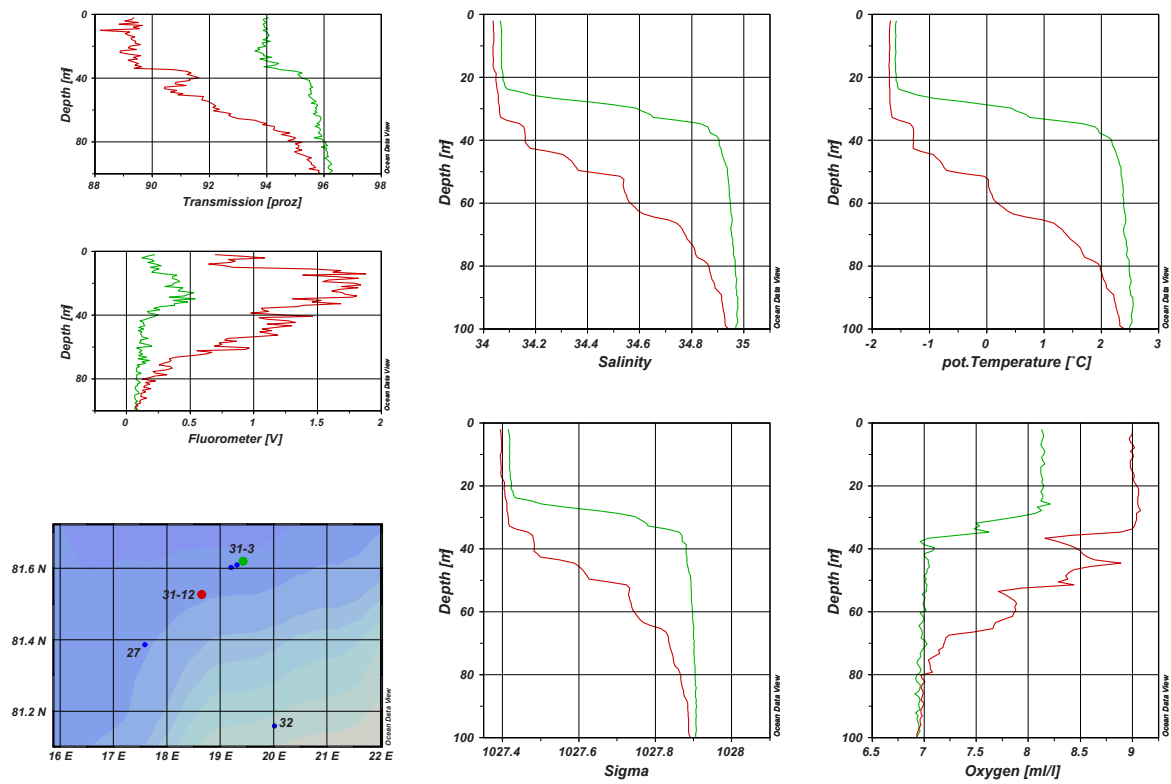


Figure A7. Overview of two of the CTD/RO casts made at station 31, on the Barents Sea shelf-break (map, lower left corner). Profiles shown for the upper 200m of the water column: transmission (in proz), fluorescence (in V), salinity, potential temperature (in °C), sigma (sea water density), and oxygen concentration (in ml l<sup>-1</sup>). Cast 31-3 was sampled. Note difference in profiles, especially for fluorescence, salinity and temperature, between the casts during this sea ice station.